RELIABILITY OF REINFORCED CONCRETE BEAMS IN TORSION

by

Salman K. Mir

Thesis submitted to the Faculty of the

Virginia Polytechnic Institute and State University

in partial fulfillment of the requirements for the degree of

MASTER OF SCIENCE

in

Civil Engineering

APPROVED:

Kamal B. Rojiani, Chairman

Richard M. Barker

Don A. Garst

July, 1985

Blacksburg, Virginia

RELIABILITY OF REINFORCED CONCRETE BEAMS IN TORSION

by

Salman K. Mir

(ABSTRACT)

The level of safety associated with the ACI Standard 318-83 design criteria for torsional reinforced concrete members is evaluated. Advanced first-order, second-moment reliability analysis is used to compute the reliability index. Reinforced concrete beams, subjected to both equilibrium and compatibility torsion, are analysed. The uncertainties associated with the various torsion design parameters are included in the reliability based formulation.

For beams designed to carry equilibrium torsion, reliability indices ranging from 3.10 to 3.65 are obtained. The reliability indices for the compatibility torsion designs, analysed in this study, vary from 1.88 to 2.09. For a given beam section, the reliability index is found to decrease with increase in beam reinforcement. When the live load is reduced for members having a load influence area greater than 400 ft^2, the reliability index is found to increase with increase in basic live load to nominal dead load ratio.

ACKNOWLEDGEMENTS

I appreciate the guidance, which I received during this study, from my thesis advisor, Dr. Kamal B. Rojiani. He spent a considerable amount of time in reviewing and correcting this manuscript.

I wish to thank Prof. Richard M. Barker and Prof. Don A. Garst for accepting to serve as members of the committee, and for the suggestions that they gave me after their careful review of this manuscript.

I gratefully acknowlege the love and friendship which I have always received from my family and friends during my pursuit of education. While undertaking this study, their support was invaluable and means much to me.

TABLE OF CONTENTS

ABSTRACT ii

ACKNOWLEDGEMENTS iii

Chapter page

I. INTRODUCTION 1

PURPOSE AND SCOPE OF STUDY 5
ORGANIZATION 7

II. REVIEW ON TORSION 9

TYPES OF TORSION 9
TORSION STRESSES 10
TORSIONAL STRENGTH OF REINFORCED CONCRETE . . 13
ACI CODE CRITERIA FOR TORSION 14
TORSIONAL REINFORCEMENT 16

III. RELIABILITY ANALYSIS 18

CALCULATION OF FAILURE PROBABILITY 18
FIRST-ORDER, SECOND-MOMENT ANALYSIS 21
EQUIVALENT NORMAL DISTRIBUTIONS 31
NUMERICAL ALGORITHM 32
ANALYSIS OF UNCERTAINTIES 33

IV. EVALUATION OF UNCERTAINTIES 36

UNCERTAINTIES IN VARIABLES FOR TORSION DESIGN . 36

V. ASSESSMENT OF RELIABILITY 42

LIMIT STATE FUNCTION FOR TORSION 42
DATA DESCRIPTION 43
RESULTS AND DISCUSSION 44

VI. SUMMARY AND CONCLUSIONS 70

SUMMARY 70
CONCLUSIONS 71

REFERENCES 73

Appendix

page

A. CALCULATION DETAILS 76

CALCULATION DETAILS OF DESIGN NO. 1 76
CALCULATION DETAILS OF DESIGN NO. 7 80

VITA 90

LIST OF TABLES

Table

page

4.1. Uncertainties in Basic Variables 41

5.1. Mean Values of Variables and Reliability Indices for Equilibrium Torsion 60

5.2. Mean Values of Variables and Reliability Indices for Compatibility Torsion 61

5.3. Variation of Reliability Index with Equilibrium Torque 62

5.4. Variation of Reliability Index with Ratio L_o/D_n for Equilibrium Torsion 64

5.5. Variation of Reliability Index with Compatibility Torque 66

5.6. Variation of Reliability Index with Ratio L_o/D_n for Compatibility Torsion 68

A.1. Results for Design No. 1 81

A.2. Results for Design No. 7 89

LIST OF FIGURES

Figure

page

2.1. Computation of $\Sigma b^2 h$ for some Typical Beam Cross Sections . . 11

3.1. Effect of Relative Positions and Dispersions of $f_R(r)$ and $f_S(s)$ on P_f 20

3.2. Failure Criterion for a Univariate Limit State 23

3.3. Failure Criterion for a Bivariate Limit State 25

3.4. Limit State in Original and Reduced Coordinates 29

5.1. Design No. 1, Source: Ref. [22] 48

5.2. Design No. 2, Source: Ref. [33] 49

5.3. Design No. 3, Source: Ref. [15] 50

5.4. Design No. 4, Source: Ref. [26] 51

5.5. Design No. 5, Source: Ref. [27] 52

5.6. Design No. 6, Source: Ref. [32] 53

5.7. Design No. 7, Source: Ref. [26] 54

5.8. Design No. 8, Source: Ref. [8] 55

5.9. Design No. 9, Source: Ref. [9] 56

5.10. Design No. 10, Source: Ref. [27] 57

5.11. Design No. 11, Source: Ref. [22] 58

5.12. Design No. 12, Source: Ref. [27] 59

5.13. Effect of Reinforcement, A_t/s, on Reliability Index for Equilibrium Torsion 63

5.14. Effect of Ratio L_o/D_n on Reliability Index for Equilibrium Torsion 65

5.15. Effect of Reinforcement, A_t/s, on Reliability Index for Compatibility Torsion 67

5.16. Effect of Ratio L_o/D_n on Reliability Index for Compatibility Torsion 69

6.1. Shear and Torque Diagrams for Design No. 1 77

6.2. Moment Distribution for Design No. 7 83

6.3. Shear and Torque Diagrams for Design No. 7 84

Chapter I

INTRODUCTION

Engineering analyses and designs, under most circumstances, are based on incomplete information and thus involve uncertainties. In view of these uncertainties, there is always some measure of risk involved in engineering systems. Present codes use safety factors to accomodate these uncertainties in the design process.

The design of structural systems involves the resolution of uncertainties. These uncertainties arise due to randomness in loading and structural resistance as well as due to errors in the prediction of load and resistance models. Regardless of how conservative a structural design, there is at least some risk of failure. It would not be economically feasible to design and build a structure with a zero risk of failure. It is more realistic to develop engineering designs for a certain permissible risk level and make provisions for the evaluation of this risk level.

To include the effect of uncertainties involved in structural design, current building codes use safety factors which are based primarily on engineering judgement and past experience with similar structures [31]. Some criteria, such as the Load and Resistance Factor Design, use separate coefficients for load and resistance variables for a proper representation of uncertainties associated with these variables. Because of the random variation pertaining to the values of loads and resistances, the factor of safety, which is used in the current codes as a constant number, is non-deterministic. As a result of recent research efforts, considerable statistical data is now available about loads and their behavior. The traditional methods of safety analysis cannot adequately incorporate the new information in the design formulation. Some other disadvantages of a deterministic code format are:

1. The actual risk, or the level of safety, cannot be determined.
2. The level of safety varies for different design situations.
3. The effects of randomness in the material properties and the loading are not explicitly included.

Due to the random nature of the load and resistance variables, structural problems are non-deterministic. It is rational to use a probabilistic approach for the analysis of structural safety. Probabilistic methods can be used for a systematic analysis of uncertainties and give a better representation of reality than is possible using current deterministic procedures. An analysis which uses probabilistic methods as its basis is termed "reliability based analysis".

New research and the use of computers has led to more refined methods of structural analysis. This improvement in structural analysis has not always been followed by improvements in design procedures, which are based on the use of safety factors that can no longer be justified in the presence of the new statistical data available on loads and resistances.

Theoretical concepts of reliability analysis have existed for many years and their significance in structural safety and design is recognized by the civil engineering profession. However, the implementation of these concepts in actual practice has been limited. In recent years, considerable effort has been devoted towards the development of reliability based structural design formats which are statistically consistent and exhibit explicit risk measures.

The pioneering work in the probabilistic treatment of structural safety was mainly done by Freudenthal [16,17,18] and Pugsley [28]. Freudenthal first presented the basic concepts of structural reliability analysis in 1947 [16]. A paper was published by Freudenthal, Garrelts, and Shinozuka [19] dealing with the state of art of classical reliability upto the year 1964. In 1969, Ang and Amin [2] presented a probabilistic formulation of structural safety. They proposed an extended reliability concept and discussed the sensitivity of the failure probability to the assumed distributions of the load and resistance variables. In a later paper Ang [1] proposed bases for risk evaluation and presented a reliability-based design formulation. Ang and Cornell [3] developed a safety index format and discussed the systematic analysis and evaluation of uncertainties in load and resistance variables. They also presented a formulation of practical design criteria.

Cornell [6] discussed the advantages of a probabilistic approach and presented a consistent first order reliability code format based on first and second moments of all stochastic variables involved. He gave a numerical illustration of the application of first-order, second-moment format to reinforced concrete design. Lind [23] developed consistent partial safety factors through the use of second-moment theory. He also showed that probabilistic code formats can be made equivalent to the existing code formats. Hasofer and Lind [21] proposed an invariant second-moment code format which is independent of the mechanical formulation of the failure criterion. Siu, Parimi, and Lind [30] presented an approach to code calibration to facilitate the transition from the existing code formats to the proposed probabilistic format.

Many papers have also been written on the application of probabilistic methods to reinforced concrete design in particular. Costello and Chu [7] calculated failure probabilities of singly and doubly reinforced concrete beams. Ravindra, Lind, and Siu [29] developed a reliability-based design criteria for reinforced concrete in flexure. Ellingwood and Ang [13] presented a risk-based evaluation of reinforced concrete beams in bending and shear. Ellingwood [10] also evaluated the risk levels implied in ACI Standard 318-77 design criteria for reinforced concrete. All the above papers on reliability-based reinforced concrete design have also attempted to evaluate the uncertainties in the various parameters involved in reinforced concrete design. These parameters are called basic variables and contribute to the randomness in structural resistance.

1.1 PURPOSE AND SCOPE OF STUDY

Considerable effort has been devoted to the development of reliability-based design and the statistical treatment of loads and structural materials. Methods have been developed for systematic evaluation of uncertainties in the design parameters and the risks associated with various designs. These methods provide a basis for a comparison of different design alternatives and the formulation of a consistent code format. The development of a design code is a gradual process and it is desirable that subsequent revisions bear resemblence to the criteria which already exist.

To assure continuity between proposed reliability-based design criteria and the provisions of the existing deterministic code, the reliability based code format should be aimed at providing the same risk level as obtained by deterministic designs. It is, therefore, desirable to evaluate the risks implicit in current designs. Ellingwood and Ang [13] evaluated the risks associated with reinforced concrete members designed in accordance with ACI procedures. They evaluated failure probabilities for reinforced concrete beams subjected to bending and shear. In a separate paper, Ellingwood [10] evaluated implied risk levels in reinforced concrete designs governed by ACI Standard 318-77. He evaluated safety indices for reinforced concrete beams in shear and flexure and also for tied and spirally reinforced concrete columns.

The subject of torsion design in concrete has gained serious interest due to the irregular shape of members which have been introduced by modern architecture. The use of high strength materials has led to a reduction in member sizes thus lowering their stiffnesses as well. The practice of designing reinforced concrete members in torsion is relatively new and the effects of torsion on reinforced concrete are not as well understood as is the behavior of reinforced concrete in shear and flexure. Even with the use of simplifying assumptions, modeling the torsional behavior of a heterogeneous material like reinforced concrete has been a relatively complex task. The resulting design equations for torsion involve a larger number of design parameters as compared with those in shear and flexure.

The purpose of this study is to evaluate the implied risk level for torsional reinforced concrete beams designed in accordance with ACI Standard 318-83. The evaluation of safety index underlying current designs is a necessary first step in the subsequent development of reliability based design criteria.

In this study, the advanced first-order, second-moment procedure [3,6] is used to evaluate the risk level implicit in the ACI torsion design criteria. This procedure has the advantages of being feasible and sufficiently accurate. It has been assumed that no correlation exists between various load and strength variables, that is, they are statistically independent. Statistics concerning means and coefficients of variation of the basic variables have been obtained from Refs. [11,13,24,25,31]. Assumptions have been made in the case of variables on which no statistical data was available. The computation of the safety index is based on an iterative procedure and an existing computer program was modified to meet the specific needs of this study.

Reliability indices are computed for statically determinate and indeterminate beams subjected to torsional loading. The effect of torque and basic live load to nominal dead load ratio on the reliability index is also determined.

1.2 ORGANIZATION

A brief review of torsion and the ACI Standard 318-83 provisions for the design of torsional reinforced concrete members is given Chapter 2. The difference between equilibrium and compatibility torsion is discussed and the design formulae for the two types of torsion are given. The formulation of reliability analysis is presented in Chapter 3 along with a method for the analysis of uncertainties. The reliability analysis procedure is summed up in the form of a numerical algorithm, which is used for the computation of reliability index. Chapter 4 includes the detailed evaluation of uncertainties associated with the basic variables involved in the limit state design for torsion. The application of reliability analysis to torsion and the data used for the assessment of risk in torsional reinforced concrete beams is presented in Chapter 5. The data consists of twelve practical design examples collected from different published sources. The first six examples are beams designed to carry equilibrium torque, while ACI provisions for moment redistribution govern the designs in the last six examples. A summary of results and some conclusions drawn from the reliability analysis of reinforced concrete members in torsion are presented in Chapter 6.

Chapter II

REVIEW ON TORSION

Reinforced concrete members in buildings and other structures, such as bridges, are often subjected to torsion in combination with bending and shear. When the working stress design method was in use, safety factors were large enough to accomodate the torsional stresses not considered in design. In the presently accepted ultimate strength design method, safety factors have been reduced due to a more refined analysis and the effects of torsion can no longer be ignored. Torsion has also become a common problem due to size and shape of the structural members being designed these days. With the use of high strength materials, member sizes have become smaller with considerably lower torsional stiffnesses. Also, modern architecture has introduced structures with out of plane loadings, curved beams, skew structures, and many other irregular shapes in which design for torsion is important.

2.1 TYPES OF TORSION

Torsion can be classified into two types:

1. Equilibrium torsion
2. Compatibility torsion

In the case of equilibrium torsion, the torsional moment can be determined from statics alone and all of it must be resisted to keep the structure in equilibrium. Compatibility torsion can be determined by satisfying deformational compatibility at the joints of the interconnecting members . Compatibility torque can be reduced by the redistribution of forces and moments after the cracking of concrete.

2.2 TORSION STRESSES

For members with solid circular sections, the maximum torsion stresses can be approximately calculated by using the theory of elasticity [22]:

$$\nu_{t_u} \approx 3T_u/\Sigma b^2 h \tag{2.1}$$

In the above equation, T_u is the ultimate torque and b, h are the shorter and longer dimensions, respectively, of the component rectangles into which a beam cross-section may be divided. This expression is only accurate when h is considerably larger than b. Fig. 2.1 shows the determination of $\Sigma b^2 h$ for different beam cross-sections. In Fig. 2.1(a), the value $\Sigma b^2 h$ can be simply calculated. In Fig. 2.1(b), $\Sigma b^2 h$ is calculated for the web rectangle extending to the top of the flange plus the flange rectangle whose effective width is limited to three times its thickness. Fig. 2.1(c) shows a T-beam with torsional reinforcement in both the web and the flange. In this case $\Sigma b^2 h$ will be the larger of (1) $\Sigma b^2 h$ for the web rectangle extending up to the top of flange plus $\Sigma b^2 h$ for the full width of overhanging rectangles or (2) $\Sigma b^2 h$ for the web rectangle below the flange plus $\Sigma b^2 h$ for the full flange rectangle.

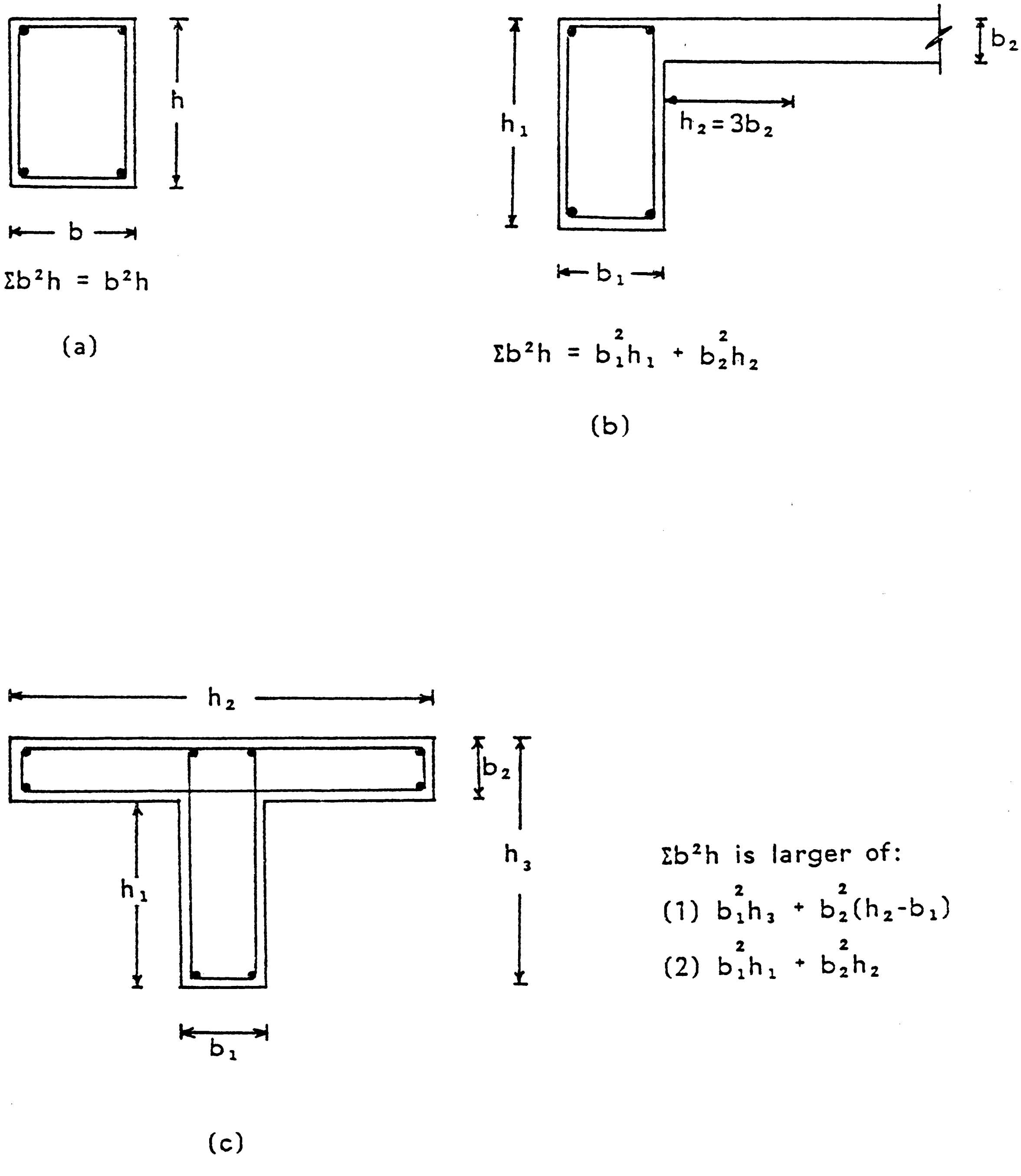

Figure 2.1: Computation of Σb^2h for some Typical Beam Cross Sections

For box sections, whose wall thickness h is at least equal to b/4, the torsion stresses can be calculated by the same equation as for solid rectangular sections. If wall thickness is less than b/4, Eq. 2.1 is modified by a multiplication factor of b/4h:

$$\nu_{t_u} = (b/4h)(3T_u/\Sigma b^2 h) \qquad \text{for } b/10 < h < b/4 \qquad (2.2)$$

Wall thicknesses less than b/10 are usually avoided because of their low buckling strength.

Diagonal shear stresses result on all faces of a member subjected to torsion. Torsion stresses add to the shear stresses on one side of the member and subtract from them on the other side. If a member is loaded to failure, it cracks and fails along 45° spiral lines due to diagonal tension caused by torsion. Critical torsional stresses will usually occur where the shear stresses are maximum and bending moments are low. Therefore, for design purposes, the interaction of shear and torsion is particularly important.

ACI committee 438 [22] estimated a value of $6.0\sqrt{f'_c}$ for the torsional stress at which cracks start to develop in a plain concrete member. This is called the "cracking stress". If torsional stresses are less than about $1.5\sqrt{f'_c}$, they have negligible effect on the strength of a member. If the torsion stress is higher than $1.5\sqrt{f'_c}$, reinforcement should be provided to prevent torsional failure. Substituting this value of $1.5\sqrt{f'_c}$ for ν_{t_u} in Eq. 2.1:

$$T_u = \phi(0.5\sqrt{f'_c}\Sigma b^2 h) \tag{2.3}$$

where ϕ=0.85 is the capacity reduction factor. The above Eq. 2.3 gives the limiting value of T_u above which torsion must be considered while designing a reinforced concrete member. In most interior reinforced concrete members of a building, torsional moments are lower than this limiting value and can be neglected. This greatly facilitates the design procedure.

2.3 TORSIONAL STRENGTH OF REINFORCED CONCRETE

The nominal torsional strength of a reinforced concrete member is the sum of the torsional strengths provided by the concrete and the torsional reinforcement, that is

$$T_n = T_c + T_s \tag{2.4}$$

For solid rectangular sections, the torsional moment strength provided by concrete is given by [22]:

$$T_c = (b^2h/3)(2.4\sqrt{f'_c}) \tag{2.5}$$

The torsional strength contributed by torsional reinforcement can be calculated using the formula [22]:

$$T_s = (\alpha_t x_1 y_1 A_t f_y)/s \tag{2.6}$$

where:

$\alpha_t = 0.66 + 0.33y_1/x_1 \leq 1.5$

x_1 = shorter dimension of stirrups measured center to center

y_1 = longer dimension of stirrups measured center to center

A_t = area of one leg of stirrup resisting torsion

f_y = yield strength of torsional reinforcement

s = stirrup spacing

Substituting the values of T_c and T_s in Eq. 2.4, the nominal torsion strength of a rectangular reinforced concrete member is given by:

$$T_n = (2.4\sqrt{f'_c})b^2h/3 + \alpha_t x_1 y_1 f_y A_t/s \tag{2.7}$$

For flanged sections, having T, L or I shapes, the total torsional strength will be the sum of the torsional strength of all the rectangular components.

2.4 ACI CODE CRITERIA FOR TORSION

When the factored torsioal moment, $T_u = \phi T_n$, exceeds $\phi(0.5\sqrt{f'_c}\Sigma b^2h)$, torsion effects must be considered along with bending and shear. ACI code [5] formula for torsion in interaction with shear is

$$T_u = \phi T_n = \phi(T_c + T_s) \tag{2.8}$$

where

$$T_c = \frac{0.8\sqrt{f'_c}\Sigma b^2h}{[1+(0.4V_u/C_tT_u)^2]^{1/2}} \tag{2.9}$$

in which $C_t = b_w d/\Sigma b^2 h$. In combined shear and torsion, the maximum permissible torsional moment for a beam to prevent overreinforcement is given by:

$$T_{n,max.} = \frac{4\sqrt{f_c}\Sigma b^2 h}{[1+(0.4V_u/C_t T_u)^2]^{1/2}} \quad (2.10)$$

The above formula corresponds to a concrete stress of 12 $\sqrt{f'_c}$ in torsion and is equal to five times the amount of torsion resisted by concrete, that is $T_{n,max.} = 5T_c$. Therefore

$$T_s + T_c \leq 5T_c \quad (2.11)$$

In addition to the above criteria, ACI code gives the following torsional limit design formula for beams which undergo compatibility torsion:

$$T_u = \phi(4\sqrt{f'_c}\Sigma b^2 h/3) \quad (2.12)$$

The above expression provides only sufficient reinforcement in a member so that it has the ductility to rotate and allow the redistribution of moments to other members in an indeterminate system. It also simplifies the otherwise lengthy procedure of computing the relative stiffnesses of the interconnecting members to determine how moments should be distributed within them. However, if stiffness analysis is used to calculate the torsional moment and it gives a value lower than the value of T_u obtained by Eq. 2.12, then stiffness analysis may be used for the design of a member subjected to torsion.

2.5 TORSIONAL REINFORCEMENT

Torsion causes stresses to be induced in all faces of a member and, therefore, torsional reinforcing should be provided in all faces. The stirrups must be closed either by bending their ends around a longitudinal bar or by welding them. The yield strength of stirrup steel should not exceed 60000 psi and stirrup spacing should be limited to the lower of the values: d/2, $(x_1+y_1)/4$, or 12 in. to control crack widths.

ACI code requires that the combined web reinforcement for shear and torsion must meet the following minimum value:

$$2A_t/s + A_v/s \geq 50b_w/f_y \tag{2.13}$$

in which A_v is the area of two legs of a closed stirrup and A_t is the area of one leg of a closed stirrup. The values of A_v and A_t can be determined as follows:

$$A_v = V_s s/df_y \tag{2.14}$$

$$A_t = T_s s/(\alpha_t x_1 y_1 f_y) \tag{2.15}$$

The torsional longitudinal steel is determined by satisfying the moment equilibrium and assuming that the yield strengths of both the web and the longitudinal reinforcing are the same [22]:

$$A_\ell = 2A_t(x_1+y_1)/s \tag{2.16}$$

This longitudinal steel is added to the steel required for resisting flexure. The minimum amount of longitudinal reinforcement which must be provided is given by:

$$A_\ell = \frac{T_u}{[T_u - V_u/3C_t]} 400bs/f_y - 2A_t(x_1+y_1)/s \qquad (2.17)$$

where $2A_t \geq 50b_w s/f_y$. There must be a longitudinal bar in every corner of the section and additional longitudinal bars may be placed in between the corner bars to produce a cage. The strength of closed stirrups cannot be developed without this additional longitudinal reinforcing.

Chapter III

RELIABILITY ANALYSIS

Since both loads and resistances are random, a rational approach would be one which incorporates the random nature of the load and resistance variables in the analysis and design procedure. As opposed to the current deterministic procedures, probabilistic analysis and design allows us to include the effects of randomness associated with loads and resistances.

3.1 CALCULATION OF FAILURE PROBABILITY

If the structural resistance and load effect are represented by R and S, respectively, then failure is the event that load effect exceeds the structural resistance. The probability of failure is defined as the probability that the resistance is less than the load effect, that is, P(R<S). It has been shown [18,19] that, for statistically independent R and S, the probability of failure can be computed as

$$P(R<S) = P_f = \int_0^{\infty} F_R(s) f_S(s) ds \qquad (3.1)$$

in which $f_S(s)$ is the probability density function of the loads and $F_R(s)$ is the cumulative distribution function for the resistance, R, evaluated at r = s. If both the structural resistance and load effect are assumed to be normally distributed, or lognormally distributed, then the probability of failure can be easily determined using standard procedures. For example, if R and S are assumed to be normal variates, then:

$$P_f = \phi[-(\mu_R-\mu_S)/[\mu_R^2 + \mu_S^2]^{1/2}] \quad (3.2)$$

in which $\phi[\ ]$ is the standard normal probability, μ_R, μ_S = means of R and S, respectively, and σ_R, σ_S = standard deviations of R and S, respectively. If R and S both have lognormal distributions, then:

$$P_f = \phi[-\ln(\mu_R/\mu_S)/[V_R^2 + V_S^2]^{1/2}] \quad (3.3)$$

where V_R, V_S = coefficients of variation in R and S. The coefficient of variation is a convenient dimensionless measure of variability and is the ratio of the standard deviation to the mean of a variable. Eq. 3.3 is only accurate if both V_R and V_S have values less than 0.30.

Once the probability of failure is known, the reliability, or the probability of survival, can be determined from the relationship:

$$P_s = 1 - P_f \quad (3.4)$$

As illustrated by Ang [4], the probability of failure depends both on the relative positions of the probability density functions of the variables involved as well as the degree of dispersion exhibited by them. As shown by Fig. 3.1, the probability of failure increases as the curves $f_R(r)$ and $f_S(s)$ come closer together. An increase in the degree of dispersion, of either R or S, also increases the failure probability. These dispersions are commonly expressed in terms of coefficient of variations, V.

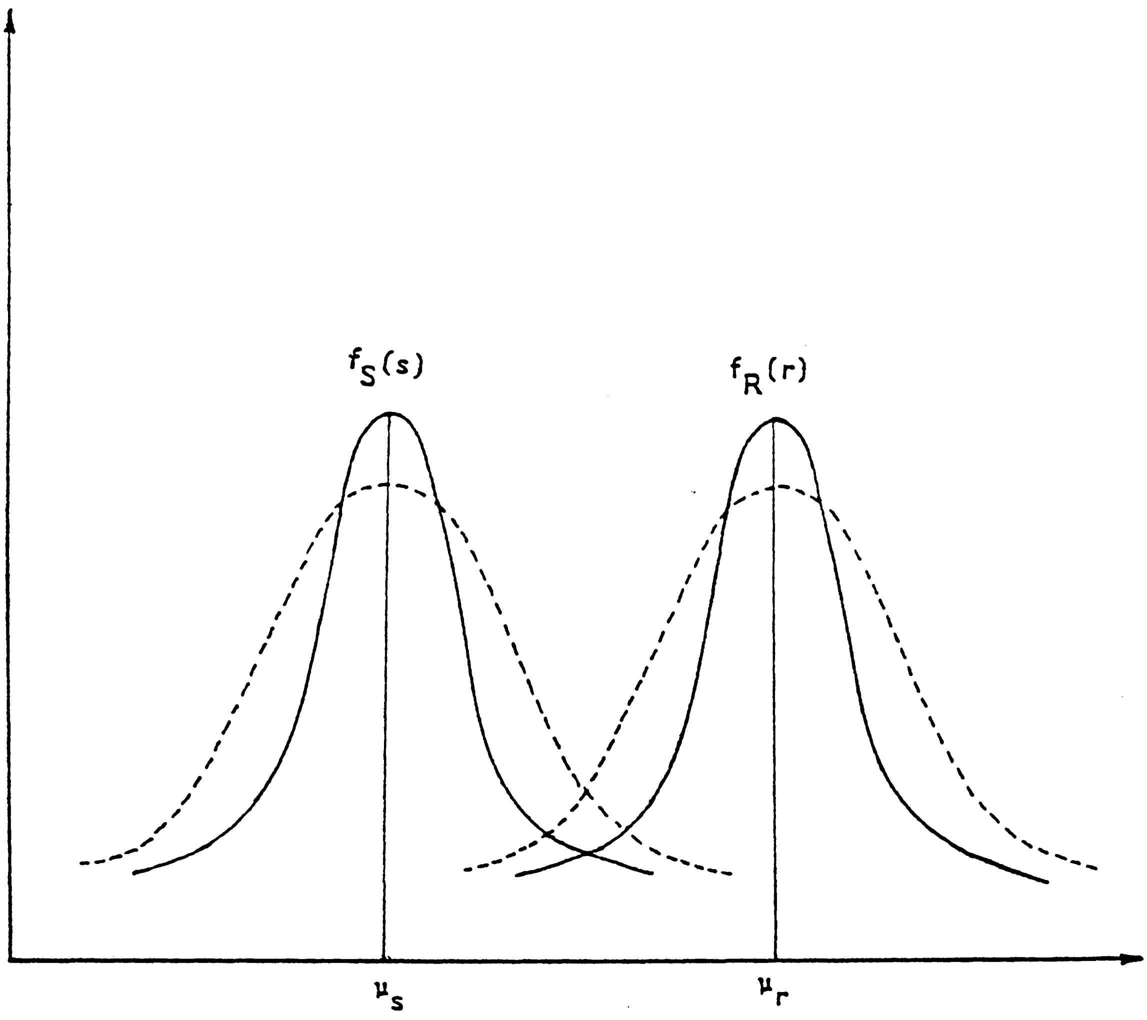

Figure 3.1: Effect of Relative Positions and Dispersions of $f_R(r)$ and $f_S(s)$ on P_f

The probability of failure also depends on the form of the distribution functions, $f_R(r)$ and $f_S(s)$. In reality, it is very difficult to determine the exact forms of the distribution functions. They can only be predicted through the use of theoretical models which are subject to errors. For high risk levels ($P_f>10^{-3}$), the calculation of failure probability is not sensitive to the form of the prescribed distribution. However, if the measure of risk involved is small ($P_f<10^{-5}$), then the accuracy of probability of failure depends on the type of distribution assumed [2,3].

3.2 FIRST-ORDER, SECOND-MOMENT ANALYSIS

An exact evaluation of the failure probability is only possible if the true distributions of the variables can be determined. In most cases, there is insufficient data available to specify the true distributions. Even if the true distributions are known, it is impractical to use them because of the resulting complexity in numerical integration involved in the calculation of failure probability through Eq. 2.1. Therefore, it is desirable to make use of approximate procedures, such as equivalent normal distributions, in reliability analysis. Available information is usually only sufficient for the evaluation of the mean values and standard deviations of the variates. These means and variances are also called the first and second moments. An approach in which only the first two moments of the variables are considered for the purpose of reliability analysis is called second-moment analysis. For many situations, second-moment analysis can be used to evaluate the reliability with sufficient accuracy. It is also possible to include the effect of non-normal distributions by transforming these distributions into equivalent normal distributions.

UNIVARIATE PROBLEM

For the purpose of illustration, let us first consider a structural member having a deterministic resistance, R. If this member is subjected to a random load, S, as shown in Fig. 3.2, then failure will occur when S>R. The design of this member will be based on the requirement that the probability of the failure event P(S>R) is less than an allowable probability of failure. That is,

$$P(S>R) < P_{f(allow.)} \tag{3.5}$$

However, since in general there is incomplete information available on the distribution of S, the failure criterion $P(S>R) < P_{f(allow.)}$ is replaced by a criterion involving only the mean and the standard deviation of S, such that

$$R \geq \mu_S + \beta\sigma_S \tag{3.6}$$

in which μ_S = the mean value of S, σ_S = the standard deviation of S, and β = the reliability coefficient. The smallest value of β satisfying the above equation is called the safety index and is a measure of reliability of the member.

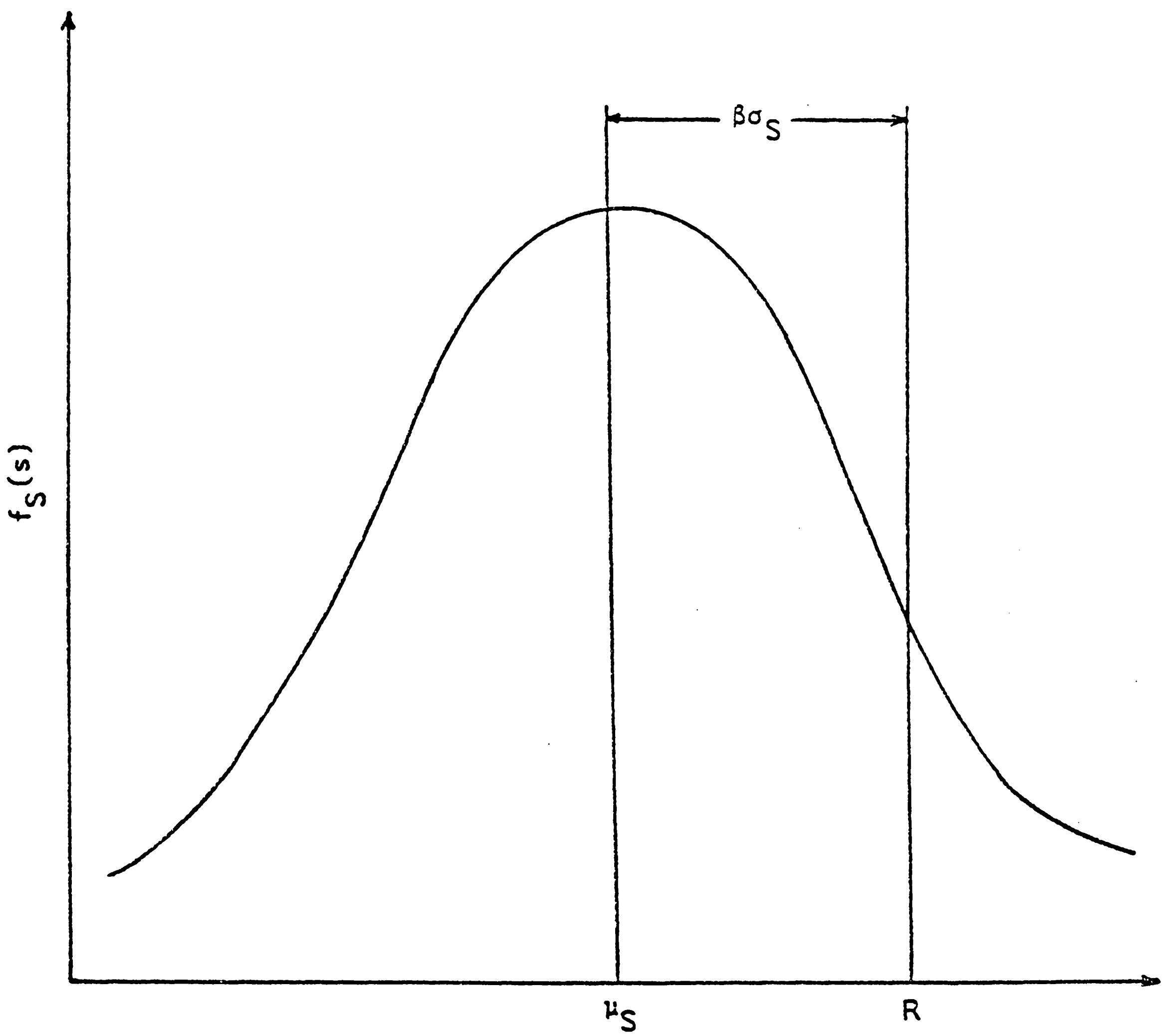

Figure 3.2: Failure Criterion for a Univariate Limit State

BIVARIATE PROBLEM

Now, suppose that both the structural resistance and load effect are statistically independent random variables. As shown in Fig. 3.3, the limit state equation $g(R,S)=0$ will divide the plane of R and S into a safe region $g(R,S) > 0$, and an unsafe region $g(R,S) < 0$. To make the measurements along the two axes comparable, transform the variables R and S into reduced variates with zero mean and unit standard deviation:

$$r = (R-\mu_R)/\sigma_R \quad \text{and} \quad s = (S-\mu_S)/\sigma_S$$

Based on the reduced variates, the failure criterion divides the plane of R and S into a safe region $g_1(r,s)$ and a failure region $g_1^*(r,s)$. For an acceptable design, the circle, with reliability index β as its radius, should lie entirely within the safe region $g_1(r,s)$.

GENERALIZATION

In general, engineering systems may involve multiple variables $X_1, X_2, \ldots, X_n$. The limit state for a multivariate system is written as

$$g(X) = g(X_1, X_2, \ldots, X_n) = 0 \tag{3.7}$$

The above equation represents a failure surface dividing the n-dimensional plane into the failure region $g(X)<0$ and the safe region $g(X)>0$. The probability of failure will be the volume integral over the failure region [4]:

$$P_f = \int \ldots \int f_{X_1, \ldots, X_n}(x_1, \ldots, x_n) dx_1, \ldots, dx_n \tag{3.8}$$

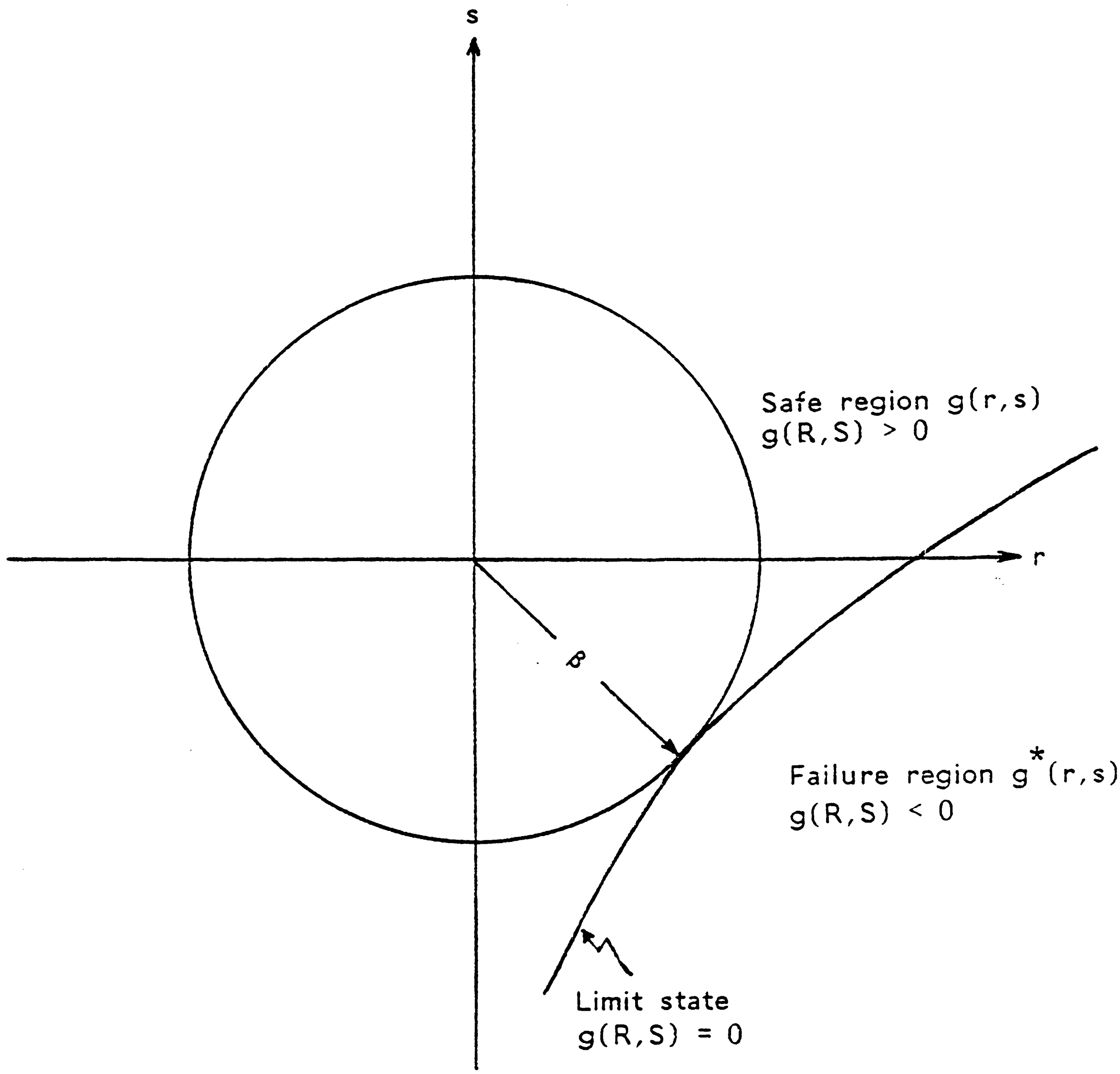

Figure 3.3: Failure Criterion for a Bivariate Limit State

in which $f_{X_1,\ldots,X_n}(x_1,\ldots,x_n)$ is the joint probability density function for the variables $X_1,\ldots,X_n$. In most cases, it is difficult to determine the joint density function of the variables involved. In fact, there may not even be enough information available on the probability density functions of individual variables and only the means and variances may be evaluated. Even if statistical data were available to define the distributions of the individual variables, it would be impractical to perform the numerical integrations required to evaluate the failure probability from Eq. 3.8. These difficulties have led to the development of first-order, second-moment (FOSM) reliability analysis methods.

If the performance function g(X) is expanded in a Taylor series at a point on the failure surface $g(X^*)=0$, then

$$g(X_1,\ldots,X_n) = g(X_1^*,\ldots,X_n^*) + \Sigma(X_i-X_i^*)(\partial g/\partial X_i) + \Sigma\Sigma(X_i-X_i^*)(X_j-X_j^*)/(\partial^2 g/\partial X_i\partial X_j) +\ldots.. \quad (3.9)$$

where the derivatives are evaluated at the linearization point $(X_1^*,\ldots,X_n^*)$. Since $g(X_1^*,\ldots,X_n^*)=0$ on the failure surface, Eq. 3.9 reduces to

$$g(X_1,\ldots,X_n) = \Sigma(X_i-X_i^*)(\partial g/\partial X_i) + \Sigma\Sigma(X_i-X_i^*)(X_j-X_j^*)/(\partial^2 g/\partial X_i\partial X_j) +\ldots.. \quad (3.10)$$

Introducing reduced variates with zero means and unit standard deviations:

$$x_i = (X_i - \mu_{X_i})/\sigma_{X_i} \tag{3.11}$$

from which

$$X_i = \sigma_{X_i} x_i + \mu_{X_i} \tag{3.12}$$

The failure surface will now be represented in the space of reduced variates, x_i, and the limit state Eq. 3.7 can be written as

$$g_1(\sigma_{X_1} x_1 + \mu_{X_1}, \ldots, \sigma_{X_n} x_n + \mu_{X_n}) = 0 \tag{3.13}$$

From Eq. 3.12,

$$X_i - X_i^* = (\sigma_{X_i} x_i + \mu_{X_i}) - (\sigma_{X_i} x_i^* + \mu_{X_i})$$

or

$$X_i - X_i^* = \sigma_{X_i}(x_i - x_i^*) \tag{3.14}$$

Also, since

$$\partial g/\partial X_i = \partial g_1/\partial x_i (dx_i/dX_i) = 1/\sigma_{X_i}(\partial g_1/\partial x_i) \tag{3.15}$$

we can write Eq. 3.10 as

$$g_1(\sigma_{X_1} x_1 + \mu_{X_1}, \ldots, \sigma_{X_n} x_n + \mu_{X_n}) = \Sigma(x_i - x_i^*)(\partial g_1/\partial x_i) + \Sigma\Sigma(x_i - x_i^*)(x_j - x_j^*)/(\partial^2 g_1/\partial x_i \partial x_j) + \ldots.. \tag{3.16}$$

Using a first-order approximation, Eq. 3.16 reduces to

$$g_1(\sigma_{X_1} x_1 + \mu_{X_1}, \ldots, \sigma_{X_n} x_n + \mu_{X_n}) = \Sigma(x_i - x_i^*)(\partial g_1/\partial x_i) \tag{3.17}$$

The mean value and the variance (for uncorrelated variates) of the function $g_1(X)$ in Eq. 3.17 is

$$\mu_{g_1} \approx -\Sigma x_i^*(\partial g_1/\partial x_i) \tag{3.18}$$

$$\sigma_{g_1}^2 \approx \Sigma \sigma_{X_i}^2(\partial g_1/\partial x_i)^2 = \Sigma(\partial g_1/\partial x_i)^2 \tag{3.19}$$

The reliability index, β, is given by the ratio μ_{g_1}/σ_{g_1} and is the distance from the tangent plane of the failure surface at x_i^* to the origin of the reduced variates [4]:

$$\beta = -\Sigma x_i^*(\partial g_1/\partial x_i)/[\Sigma(\partial g_1/\partial x_i)^2]^{1/2} \tag{3.20}$$

In the mean value FOSM method, the failure function is linearized at the mean values of the variables X_i. Studies [3,6] have shown that this can lead to significant errors when the function g(X) is non-linear. The mean point may be some distance from the non-linear failure surface g(X)=0 and the error will increase with increasing distances from the linearization point. Also, the mean value FOSM method lacks invariance and may give different results for different, but mechanically equivalent, formulations of the same problem. Both these problems can be avoided if the function g(X) is linearized at a point on the failure surface.

Fig. 3.4 shows the failure surface in original and reduced variable coordinates. The minimum distance between the failure surface g(X)=0 and the origin of the reduced variates gives a measure of the system reliability [20]. This minimum distance is called the reliability

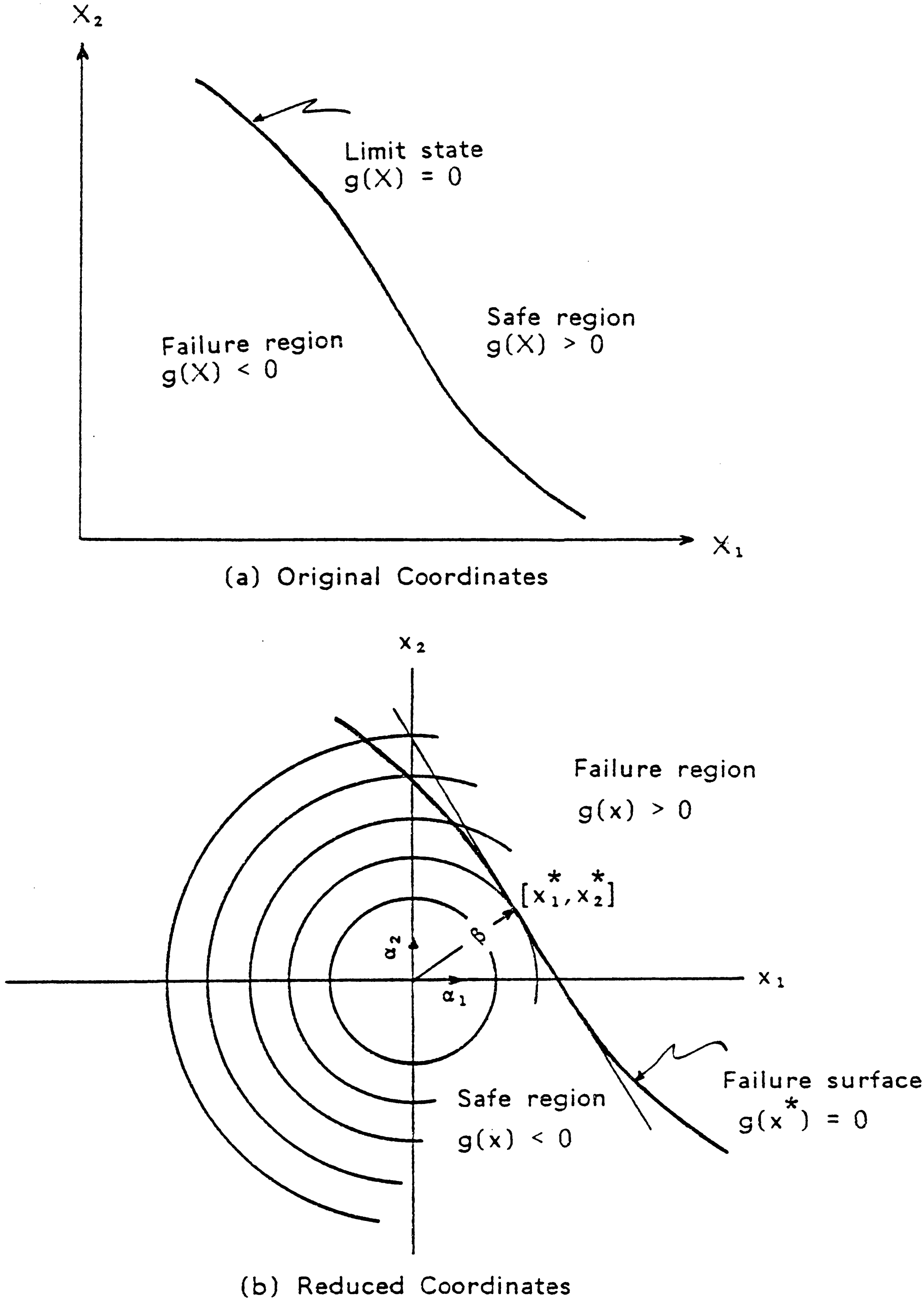

Figure 3.4: Limit State in Original and Reduced Coordinates

index, β, and the point $(x_1^*,\ldots,x_n^*)$ on the failure surface which corresponds to this minimum distance is referred to as the checking or design point. The relationship between the reliability index and the design point can be expressed as:

$$x_i^* = -\alpha_i^* \beta \tag{3.21}$$

where α_i^* are the direction cosines along the axes x_i and are given by:

$$\alpha_i^* = (\partial g_1/\partial x_i)/[\Sigma(\partial g_1/\partial x_i)^2]^{1/2} \tag{3.22}$$

In the original variable space, the design point variables are given by:

$$X_i^* = \mu_{X_i} + \sigma_{X_i} x_i^* \tag{3.23}$$

Substituting $x_i^* = -\alpha_i^* \beta$, Eq. 3.23 can be written as:

$$X_i^* = \mu_{X_i} - \alpha_i^* \beta \sigma_{X_i} \tag{3.24}$$

If the true distributions of the variables in the limit state equation are known, then there is an exact relation between reliability index, β, and the probability of failure, P_f. For example, consider the two variable problem of structural resistance, R, and load effect, S. If R and S are normal and statistically independent, then the failure probability is given by Eq. 3.2, in which

$$\beta = (\mu_R - \mu_S)/[\sigma_R^2 + \sigma_S^2]^{1/2} \tag{3.25}$$

Therefore,

$$P_f = \phi[-\beta] \tag{3.26}$$

or

$$\beta = \phi^{-1}[1 - P_f] \tag{3.27}$$

Even if the probability laws governing the basic variables are unknown, β is a useful comparative measure of reliability and is a basis for the evaluation of relative safety of various design alternatives.

3.3 EQUIVALENT NORMAL DISTRIBUTIONS

Using the advanced first-order, second-moment analysis, the evaluation of reliability index, β, through Eqs. 3.26 and 3.27 is exact only if the basic variables are normally distributed and the performance function g(X) is linear [25]. Reliability analysis of structures involves many variables with non-normal distributions. Information on probability distributions of the random variables can be included in the reliability analysis by transforming the non-normal variables into equivalent normal variables. The equivalent mean and standard deviation of the non-normal distribution can be calculated by the following relations [4]:

$$\mu_i^N = x_i^* - \sigma_{X_i}^N \phi^{-1}[F_{X_i}(x_i^*)] \tag{3.28}$$

$$\sigma_{X_i}^N = \phi\{\phi^{-1}[F_{X_i}(x_i^*)]\}/f_{X_i}(x_i^*) \tag{3.29}$$

where $\mu_{X_i}^N$, $\sigma_{X_i}^N$ = the mean value and standard deviation, respectively, of the equivalent normal distribution, and

$F_{X_i}(x_i^*)$, $f_{X_i}(x_i^*)$ = the original cumulative distribution and probability density functions, respectively, of the non-normal distribution at points x_i^* on the failure surface. Since the transformation takes place on the failure surface, the probability of failure, obtained by using the mean value and standard distribution of the equivalent normal distribution, is a good approximation of the true failure probability. The reliability index, β, can then be determined from Eq. 3.27.

3.4 NUMERICAL ALGORITHM

The numerical algorithm used for the iterative solution of the reliability index involves the following general steps [4,25]:

1. Define the appropriate limit state function using Eq. 3.7.
2. Make an initial guess at the reliability index, β.
3. Set the initial checking point values, say mean values, for all the basic variables.
4. If the performance function involves any variates with non-normal distributions, then compute the mean and standard deviation of the equivalent normal distributions, using Eqs. 3.28 and 3.29, for those variables which are non-normal.
5. Transform the original variables into reduced variates with zero mean and unit standard deviation using Eq. 3.11.
6. Define the limit state equation in the space of reduced variates using Eq. 3.13

7. Compute the partial derivatives, $\partial g_1/\partial x_i$, at points x_i^* on the failure surface.
8. Using Eq. 3.22, compute the direction cosines, α_i^*.
9. From Eq. 3.21, compute new values of checking points x_i^*. Repeat steps 4 through 9 until the estimates of α_i^* stabilize.
10. Compute the value of β satisfying the limit state equation $g_1(\sigma_{X_1} x_1 + \mu_{X_1}, \ldots, \sigma_{X_n} x_n + \mu_{X_n}) = 0$. Repeat steps 4 through 10 until the difference in the successive values of β is negligible.

3.5 ANALYSIS OF UNCERTAINTIES

Uncertainties are functions of both inherent variabilities and modeling errors. Inherent variabilities result from the properties which are intrinsic to a variable and may not be controlled. Such uncertainties generate random errors which can be treated statistically. Modeling uncertainties include errors due to imperfect predictions in the modeling of a physical process, estimation errors, and idealizations of actual loads in space and time [25]. Modeling uncertainties may contain both a systematic and a random component. The systematic error results from a bias in the prediction or estimation of a physical process, whereas the random component represents the range of error in a variable. The systematic error may be corrected by applying a constant bias factor [4] and the random error is represented by the standard deviation or the coefficient of variation.

The main difference between inherent and modeling uncertainties is that while the inherent uncertainties may not be controlled owing to their nature, modeling uncertainties can be reduced by more refined predictions of a model and the acquisition of additional data.

Let X be a random variable whose actual value is unknown. If $X^{\bullet}$ is used as a model to predict the value of X, then [4]:

$$X = NX^{\bullet} \tag{3.30}$$

where $X^{\bullet}$ has a predicted mean value $\overline{X}$, and a coefficient of variation δ_X representing the variability in $X^{\bullet}$. N is also a random variable, whose mean value, $\overline{N}$, represents the correction for the systematic error in the predicted mean value $\overline{X}$. The random component of the error in the prediction of the mean value X is represented by the coefficient of variation, Δ_X, of N.

Assuming that N and $X^{\bullet}$ are statistically independent, the mean value of the random variable X will be

$$\mu_X = \overline{N}\overline{X} \tag{3.31}$$

If the mean value of the correction factor, $\overline{N}$, is taken as unity, then Eq. 3.31 gives

$$\mu_X = \overline{X} \tag{3.32}$$

Using first-order approximation [6], the total uncertainty in the prediction of X is

$$V_X = [\delta_X^2 + \Delta_X^2]^{1/2} \tag{3.33}$$

If Y is a function of several random variables $Y_1, Y_2, \ldots, Y_n$, then

$$Y = f(Y_1, Y_2, \ldots, Y_n) \tag{3.34}$$

Y can only be approximately modeled with the application of a correction factor, N, such that

$$Y = Nf^{\bullet}(Y_1, Y_2, \ldots, Y_n) \tag{3.35}$$

where N has a mean value of unity and a coefficient of variation Δ_Y. Expanding Y in a Taylor series with respect to the mean values of the basic variables, $\mu_{Y_1}, \ldots, \mu_{Y_n}$, and ignoring the higher order terms

$$Y = Nf^{\bullet}(\mu_{Y_1}, \ldots, \mu_{Y_n}) + \Sigma(Y_i - \mu_{Y_i})(\partial Y/\partial Y_i) \tag{3.36}$$

in which the partial derivatives are evaluated at μ_{Y_i}. The predicted mean and variance of Y will then be given by

$$\mu_Y \simeq f^{\bullet}(\mu_{Y_1}, \ldots, \mu_{Y_n}) \tag{3.37}$$

$$\sigma_Y^2 \simeq \Sigma(\partial Y/\partial Y_i)^2 \sigma^2_{Y_i} + \Sigma\Sigma(\partial Y/\partial Y_i)(\partial Y/\partial Y_j)COV(Y_i, Y_j) \tag{3.38}$$

where $COV(Y_i, Y_j)$ is the covariance between Y_i and Y_j. For statistically independent random variables, the covariance of Y_i and Y_j is zero and the variance of Y reduces to

$$\sigma_Y^2 = \Sigma(\partial Y/\partial Y_i)^2 \sigma^2_{Y_i} \tag{3.39}$$

Therefore the total c.o.v. can be calculated from

$$V_Y = [\Delta_Y^2 + \Sigma(\partial Y/\partial Y_i)^2 \sigma_Y^2/\mu_Y^2]^{1/2} \tag{3.40}$$

Chapter IV

EVALUATION OF UNCERTAINTIES

The uncertainties in basic design variables are evaluated from available statistical data. If X is a basic variable, then its inherent variability will be represented by the coefficient of variation, δ_X , obtained from the data. Also, a bias factor, N, may be assigned to the predicted mean value of X to correct for modeling errors. The mean value of this bias factor is taken as unity and its coefficient of variation, Δ_X , represents the random component of the modeling error.

4.1 UNCERTAINTIES IN VARIABLES FOR TORSION DESIGN

Using a systematic analysis, as detailed in Sec. 3.5, the evaluation of inherent and modeling uncertainties leads to the computation of the total coefficient of variation. The following paragraphs present the data collected from literature, and illustrate the analysis of uncertainties involved in the design of torsional reinforced concrete members. All the variables are assumed to be statistically independent.

UNCERTAINTIES IN CONCRETE COMPRESSIVE STRENGTH

From tests conducted on standard concrete cylinders with nominal 28 day compressive strength, f'_c , of 3000 psi, the predicted mean value, $\overline{f'_c}$, was 3456 psi and the inherent variability, $\delta_{f'_c}$, was estimated to be 0.12 [13]. The predicted value of concrete strength observed under laboratory conditions can be 10% to 20% higher than the actual compressive strength of in-situ concrete. Other factors which lead to prediction errors are effects of creep, shrinkage and curing conditions. An uncertainty of 0.16 has been assumed [13] for the combined effect of the factors mentioned above. The error in predicting the mean value of concrete is estimated to be 0.07, and the total modeling error thus becomes

$$\Delta_{f'_c} = [(0.07)^2 + (0.16)^2]^{1/2} = 0.18$$

Using the values of $\delta_{f'_c}$ =0.12 and $\Delta_{f'_c}$ =0.18, the total uncertainty in concrete can be calculated as

$$V_{f'_c} = [(0.12)^2 + (0.18)^2]^{1/2} = 0.21$$

The mean value for a nominal concrete strength of 4000 psi is estimated as 4700 psi [31]. In this study, the c.o.v. for 4000 psi concrete is assumed to be the same as for 3000 psi concrete.

UNCERTAINTIES IN STEEL YIELD STRENGTH

From mill and laboratory test data, the mean value for nominal steel yield strength of 40000 psi has been estimated to be 47700 psi [13]. For Grade 60 reinforcement, a mean value of 64000 psi was estimated [24]. The error in the predicted mean value of steel yield strength is affected by the bar size and the testing procedures. To account for the variation in the bar sizes which may be used, an uncertainty of 0.04 is estimated. The predicted mean value increases with a higher rate of loading and an uncertainty of 0.05 was estimated to correct for the higher loading rates used during testing. Also, the unstable upper yield point of steel is used to determine the steel strength instead of the lower yield point and an uncertainty of 0.10 is used to account for this practice [13]. The combined effect of the above uncertainties gives a total prediction error of

$$\Delta_{f_y} = [(0.04)^2 + (0.05)^2 + (0.10)^2]^{1/2} = 0.12$$

The inherent variability in the steel yield strength is δ_{f_y} =0.09, and the total uncertainty in f_y is

$$V_{f_y} = [(0.09)^2 + (0.12)^2]^{1/2} = 0.15$$

UNCERTAINTIES IN MEMBER DIMENSIONS

Uncertainties in dimensions b, h are functions of the quality control in construction. Ellingwood [11] has estimated a total c.o.v. of $0.4/h_n$ for h, where h_n is the nominal total depth of the member. The c.o.v. for b is also taken to be the same as that of h. Ellingwood and Ang [13] have assigned values of 0.04 for the inherent variabilities in b and h (δ_b, δ_h), and 0.02 for the prediction uncertainties in b and h (Δ_b, Δ_h). The total c.o.v. for b and h is

$$V_b = V_h = [(0.04)^2 + (0.02)^2]^{1/2} = 0.045$$

UNCERTAINTIES IN SPACING OF REINFORCEMENT

The total uncertainty in the effective depth of reinforcement, d, has been estimated as $0.68/h_n$ [11]. In this study, values of 0.07 and

0.05 were used for δ_d and Δ_d, respectively [13]. The total c.o.v. of d, is calculated to be

$$V_d = [(0.07)^2 + (0.05)^2]^{1/2} = 0.086$$

The uncertainties in x_1, y_1, and stirrup spacing, s, have been assumed to be similar to those of effective depth (d) as they all involve the placement of steel. Therefore, the same c.o.v. of 0.086 is used for the above variables.

UNCERTAINTIES IN STEEL AREA

The variability in steel area is a function of the bar diameter. The prediction errors result from uncertainties in fabrication and quality control. It has been estimated [24] that the inherent uncertainty in the steel area for flexure, A_s, is δ_{A_s} =0.02 and the modeling uncertainty, Δ_{A_s} =0.03. In this study, the same uncertainties have been assumed in the steel area for torsion and the total c.o.v. for A_t is

$$V_{A_t} = [(0.02)^2 + (0.03)^2]^{1/2} = 0.036$$

UNCERTAINTIES IN DEAD AND LIVE LOADS

Uncertainties in loads result from the inherent variabilities as well as the modeling errors due to imperfect predictions in defining loads with respect to space and time [25]. It has been estimated that the mean value of dead load, D, should be taken as 1.05 times its nominal value, and a coefficient of variation V_D =0.10 should be used. These recommendations have been followed in this study.

The live load used in this study is the lifetime maximum live load. ANSI Standard A58.1-1983 requires that the nominal live load, L_n, should be reduced as the load tributary area increases. The following load reduction formula is used for this purpose:

$$L_n = L_0(0.25+15/\sqrt{A_I}) \qquad (4.1)$$

In the above equation, L_0 is the basic live load and A_I is the influence area in ft². For beams and columns, A_I is taken as 2 and 4 times the tributary area, A_T, respectively. ANSI Standard recommends that the mean value of the lifetime maximum live load should be taken equal to its nominal value, and a coefficient of variation V_L=0.25 should be used.

All the uncertainties, discussed in the preceding paragraphs, for the variables involved in torsion design of reinforced concrete members have been summarized in Table 4.1. The ratio of mean to nominal values for material strength variables have been determined from the available data. In case of variables involving member dimensions and spacing of reinforcement, this ratio has been assumed equal to unity.

TABLE 4.1

Uncertainties in Basic Variables

Variable	Mean/Nominal	c.o.v.
Concrete Strength:		
f_c: 3000 psi	1.152	0.210
4000 psi	1.175	0.210
Steel Strength:		
f_y: 60000 psi	1.067	0.150
Dead Load	1.050	0.100
Live load	1.000	0.250
Member Dimensions:		
b,h	1.000	0.045
Reinforcement Spacings:		
d, x_1, y_1, s	1.000	0.086
Steel Area:		
A_t	1.000	0.036

Chapter V

ASSESSMENT OF RELIABILITY

Advanced first-order, second-moment analysis was used to determine the reliability-index, β, associated with members designed in accordance with the ACI code torsion criteria. The numerical algorithm used for the computation of reliability index was presented in Sec. 3.4. The effect of applied torque, T_u, and basic live load to nominal dead load ratio, L_o/D_n, on reliability index was also investigated. The beam designs were obtained from published sources and consisted of beams designed both for equilibrium and compatibility torsion.

5.1 LIMIT STATE FUNCTION FOR TORSION

The performance function for the ultimate limit state design of torsion is given by:

$$g(X) = T_c + T_s - T_u \tag{5.1}$$

where T_c and T_s are the torsional resistances provided by concrete and reinforcing steel, respectively. T_u is the ultimate torque to which a member may be subjected. From Eq. 3.4, the limit state equation for this performance function can be written as:

$$T_c + T_s - T_u = 0 \tag{5.2}$$

Substituting the values of T_c and T_s from Eqs. 2.6 and 2.11, Eq. 5.1 becomes:

$$g(X) = \frac{0.8\sqrt{f'_c}(\Sigma b^2 h)}{[1+(0.4V_u/C_t T_u)^2]^{1/2}} + \alpha_t x_1 y_1 f_y A_t/s - T_u \qquad (5.3)$$

Eq. 5.3 is the general form of the performance function used in this study to compute the reliability index associated with the torsional members. In the case of equilibrium torsion, both V_u and T_u are functions of dead and live loads to which the member is subjected. But, in the case of compatibility torsion, only V_u is a function of dead and live loads while ACI code provisions limit T_u to a maximum allowable value which is a function of concrete strength and member dimensions. This limiting value of compatibility torque can be determined from Eq. 2.12. Appendix A presents in detail the calculation of V_u and T_u both for a determinate and an indeterminate beam. The computation of partial derivatives for the two types of torsion is also included in Appendix A.

5.2 DATA DESCRIPTION

The reliability index was computed for twelve beams which have been designed for torsion. These designs were obtained from different published sources. The first six beams are subjected to equilibrium torsion and, therefore, designed to carry the full factored torque. In this case, the torsional moment, T_u can be computed from statics. The last six beams are indeterminate beams and were designed according to the torsional limit design method, which allows the redistribution of moments to other members in a structural system. Details of the various beams and their design parameters are given in Figs. 5.1 through 5.12.

The ratios of mean to nominal values and the coefficients of variation used for the basic variables in the limit state function are summarized in Table 4.1. All variables are assumed to be statistically independent and normally distributed.

5.3 RESULTS AND DISCUSSION

Tables 5.1 and 5.2 list the mean values of the basic variables which were used in the computation of reliability index through the performance function of Eq. 5.3 and using the numerical algorithm in Sec. 3.4. Table 5.1 contains the data for equilibrium torsion designs. The data for compatibility torsion designs is presented in Table 5.2. The reliability indices obtained for these designs are also given in the above tables.

The results show that the safety index, β, ranges from 3.10 to 3.65 in the case of equilibrium torsion and 1.88 to 2.09 in the case of compatibility torsion. The difference in the results for the two types of torsion is due to the difference in the method used for the calculation of design torque, T_u. As mentioned in Sec. 5.1, in the case of equilibrium torsion, T_u is determined from statics and is thus a function of the applied loads. Whereas, compatibility torque is a function of concrete strength and member dimensions.

Reliability indices obtained in this study for torsional reinforced concrete members are comparable to the values obtained for other types of reinforced concrete members [10,14,20,25]. Galambos, Ellingwood and others [20] have computed reliability indices of 2.8 and 2.4 for reinforced concrete beams subjected to flexure and shear, respectively. According to Ellingwood et. al. [25], reliability indices of current reinforced concrete designs range from 2.6 to 3.2 for flexure and 1.9 to 2.4 for shear. These values were obtained for members subjected to a combination of gravity dead and live loads. Ellingwood [12] has suggested target reliability indices of 3.0 to 3.5 for members with a ductile mode of failure and values of 4.0 or higher for members which fail in a brittle manner.

An attempt was made to study the relationship between reliability index and applied torque. The effect of the ratio of basic live load to nominal dead load, L_o/D_n, on the reliability index was also investigated. The beams shown in Figs. 5.3 and 5.11 were used to study the above relationships because their section dimensions are suitable for a wide variation in applied loading.

Fig. 5.13 shows the variation of reliability index with increase in reinforcement, which corresponds to the increase in applied torque. Fig. 5.13 was obtained by using the beam shown in Fig. 5.3 with the same geometry, but, for simplicity, it was assumed that only dead load is acting upon it. As shown by Table 5.3, the reinforcement in this beam was redesigned as the torque producing load was increased in multiples of the beam self weight. The first point on the curve, m, corresponds to the reinforcement, A_t/s, beyond which minimum reinforcement requirements govern (Eq. 2.13). The last point on the curve, n, corresponds to the value of torque beyond which the section dimensions are inadequate to satisfy Eq. 2.11. The performance function of Eq. 5.3 is only valid between the points m and n. The reliability index was computed, using Eq. 5.3, for different values of A_t/s corresponding to increasing torque. From Fig. 5.13, it is seen that β first increases sharply and then starts to decrease with increasing torque. The slope of this graph is found to be a function of the ratio V_u/T_u.

Fig. 5.14 illustrates the relationship between the ratio of basic live load to nominal dead load, L_o/D_n, and reliability index, β. The same beam of Fig. 5.3 was used to investigate this relationship. The total load (beam weight plus torque producing load) was fixed at 40000 lbs. and the ratio L_o/D_n was varied from 0 to 2.00. Table 5.4 gives the beam reinforcement, A_t/s for every increment in the ratio L_o/D_n. As is the case for most beams designed to carry full torque (equilibrium torsion), the influence area for the beam of Fig. 5.3 is less than 400 ft^2 and, therefore, basic live load is not reduced. Fig. 5.14 shows that the reliability index, β, increases sharply and then falls off with the increase in L_o/D_n. The slope of this curve is also a function of the ratio V_u/T_u.

In the case of compatibility torsion, the beam of Fig. 5.11 was used to study the effect of torsional loading and the basic live load to nominal dead load ratio, L_o/D_n, on the reliability index. Tables 5.5 and 5.6 give the beam reinforcement A_t/s for different values of applied torque and ratio L_o/D_n for the beam of Fig. 5.11. The results are presented in Figs. 5.15 and 5.16, which were obtained in a manner similar to that for equilibrium torsion.

Fig. 5.15 shows the variation in reliability index, β, as the beam reinforcement is increased corresponding to the increase in applied loading. The effect of increase in loading on reliability index is more gradual in case of compatibility torsion, as compared to the case of equilibrium torsion (Fig. 5.13). This is because the design torque T_u, in compatibility torsion, is a function of section dimensions and concrete strength (Eq. 2.12) instead of applied loads. The effect of the L_o/D_n ratio on reliability index for compatibility torsion is illustrated in Fig. 5.16. In this case, the reliability index increases with increase in L_o/D_n due to the reduction allowed in basic live load when the influence area is greater than 400 ft². Similar to the case of equilibrium torsion, the change in the slopes of curves in Figs. 5.15 and 5.16 for compatibility torsion is a function of ratio V_u/T_u.

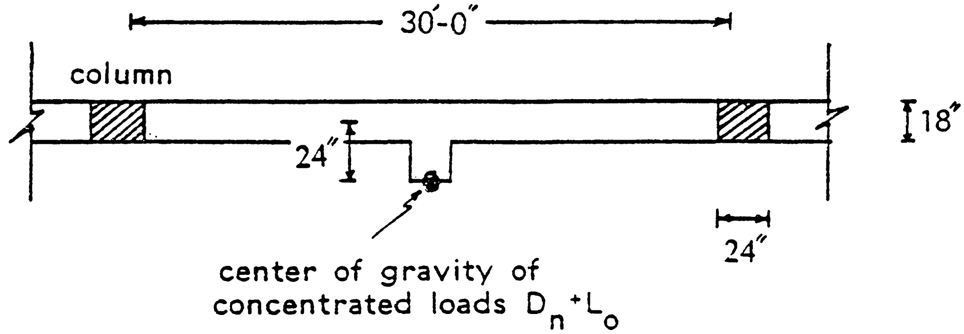

Plan

f'_c = 4000 psi
f_y = 60000 psi
L_o = 36000 lbs.
D_n = 40000 lbs.
α_t = 1.22
A_I < 400 ft², $L_n = L_o$
$V_u = 0.5(1.323D_n + L_n)$ lbs.
$T_u = 12(D_n + L_n)$ in-lbs.

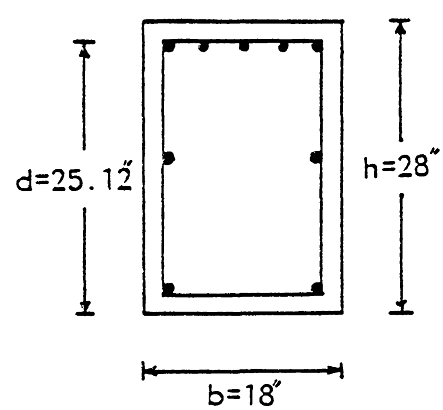

Beam Section

Figure 5.1: Design No. 1, Source: Ref. [22]

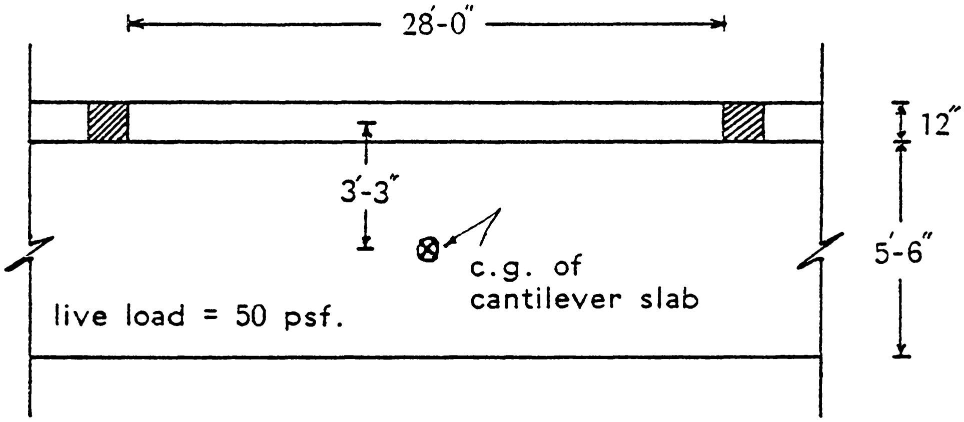

Plan

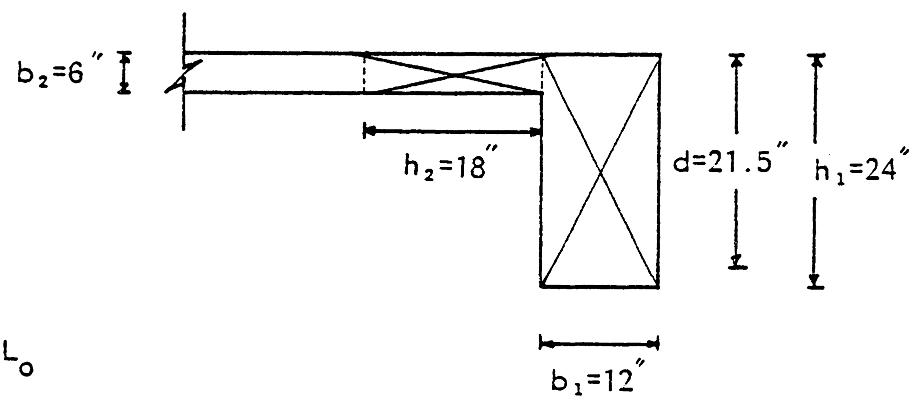

f'_c = 4000 psi
f_y = 60000 psi
L_o = 9100 lbs.
D_n = 19950 lbs.
α_t = 1.46
A_I < 400 ft², $L_n = L_o$
$V_u = 0.436(D_n + L_n)$ lbs.
$T_u = 14.39(0.684D_n + L_n)$ in-lbs.

Beam and Slab Section

Figure 5.2: Design No. 2, Source: Ref. [33]

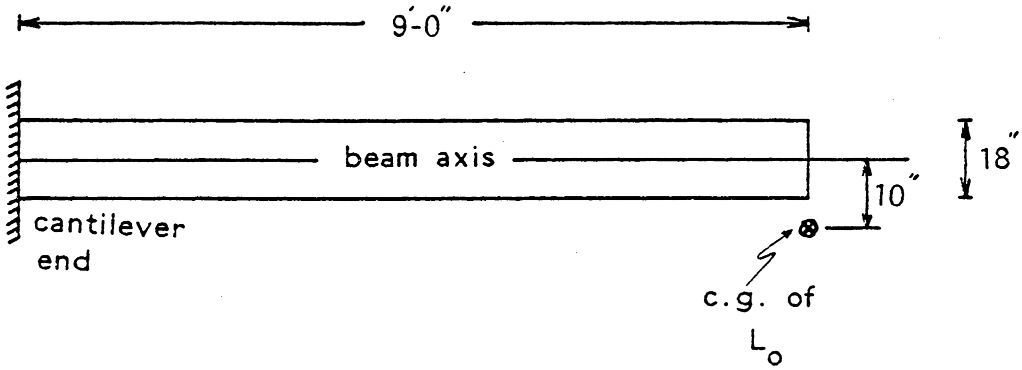

Plan

f'_c = 3000 psi
f_y = 60000 psi
L_o = 40000 lbs.
D_n = 4556 lbs.
α_t = 1.20
A_I < 400 ft^2, $L_n = L_o$
$V_u = (0.775 D_n + L_n)$ lbs.
$T_u = 10\ L_n$ in-lbs.

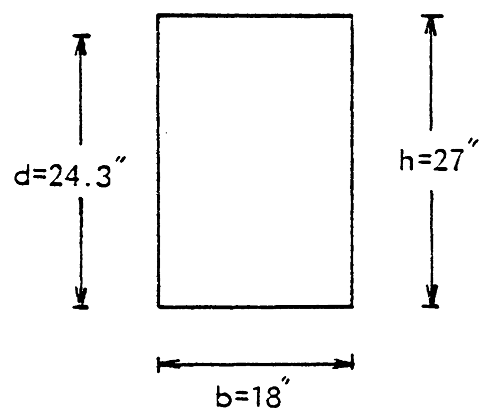

Beam Section

Figure 5.3: Design No. 3, Source: Ref. [15]

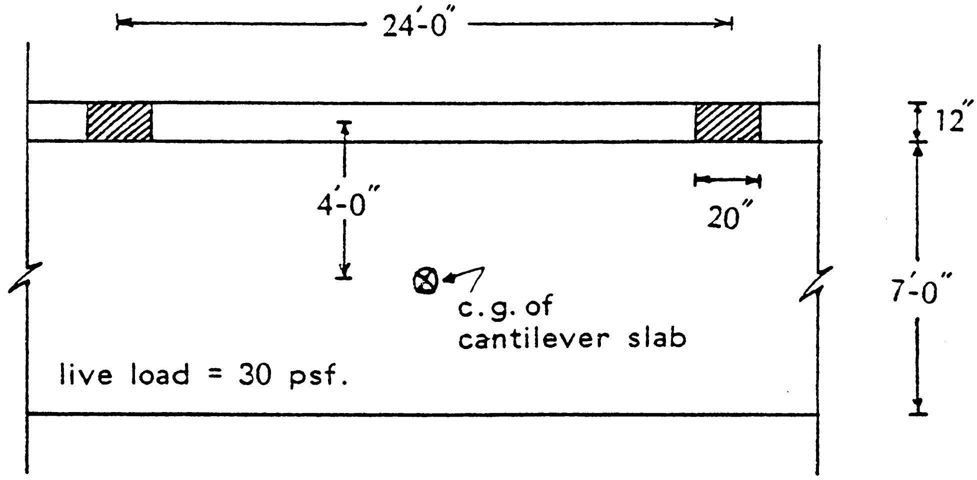

Plan

f'_c = 4000 psi
f_y = 60000 psi
L_o = 5760 lbs.
D_n = 22800 lbs.
α_t = 1.30
$A_I < 400\ ft^2$, $L_n = L_o$
$V_u = 0.405(D_n + L_n)$ lbs.
$T_u = 17.0(0.842D_n + L_n)$ in-lbs.

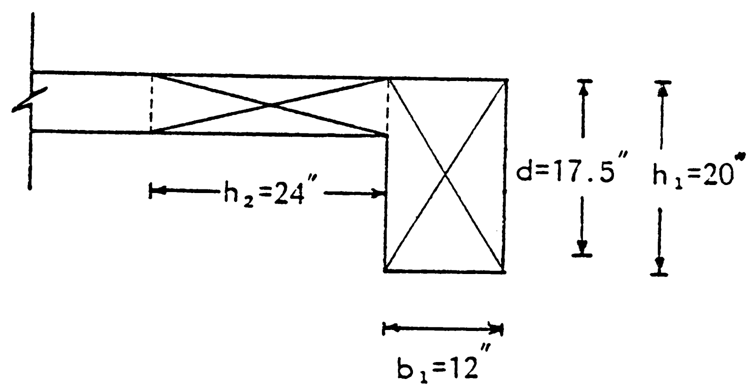

Beam and Slab Section

Figure 5.4: Design No. 4, Source: Ref. [26]

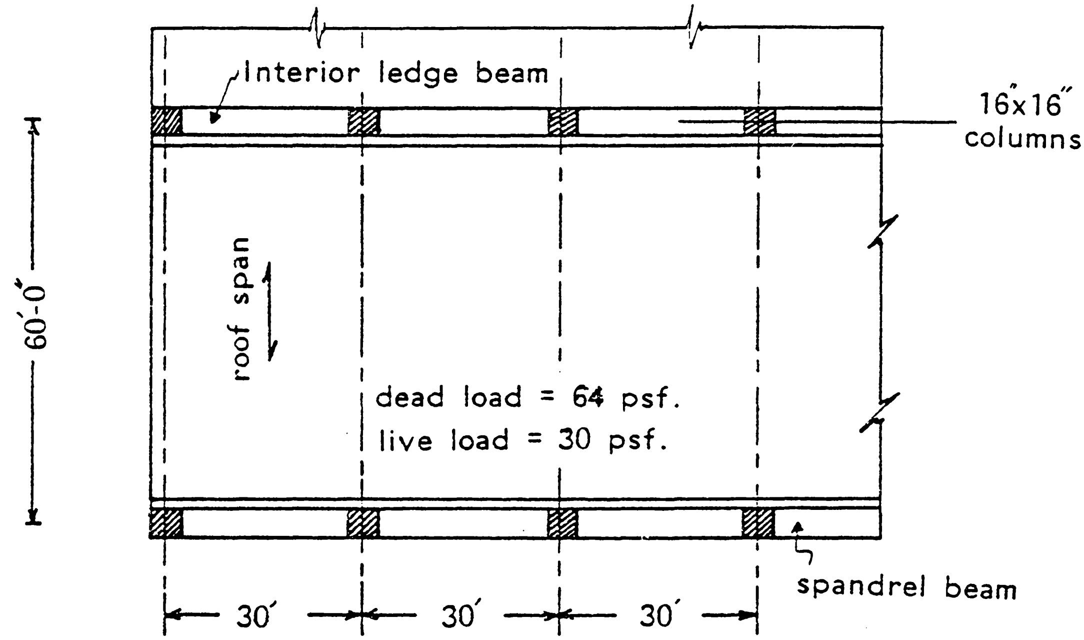

Plan

f'_c = 4000 psi

f_y = 60000 psi

L_o = 27000 lbs.

D_n = 75100 lbs.

α_t = 1.40

Live load not to be reduced for roof members, $L_n = L_o$

$V_u = 0.396(D_n + L_n)$ lbs.

$T_u = 4.354(0.767D_n + L_n)$ in-lbs.

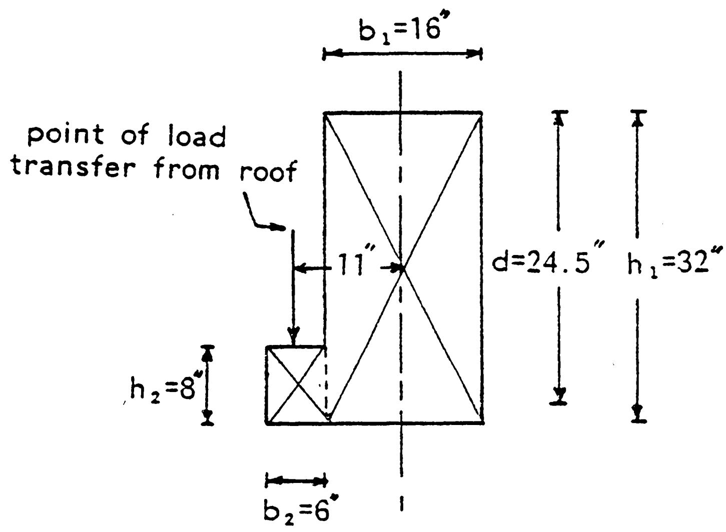

Spandrel Beam Section

Figure 5.5: Design No. 5, Source: Ref. [27]

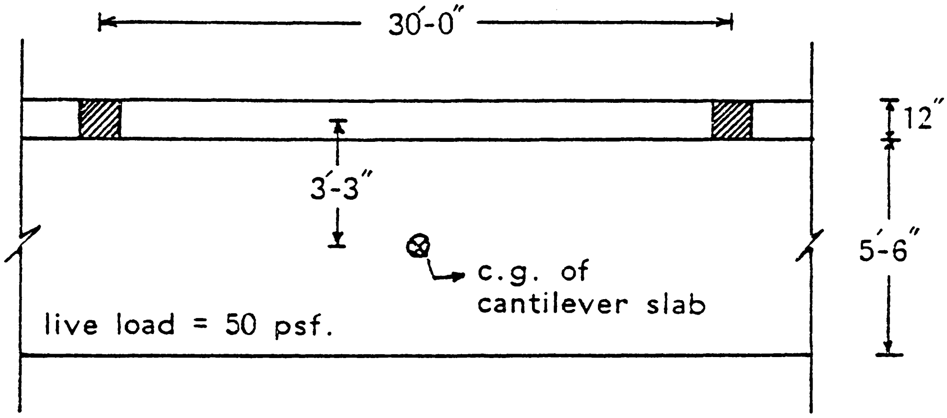

Plan

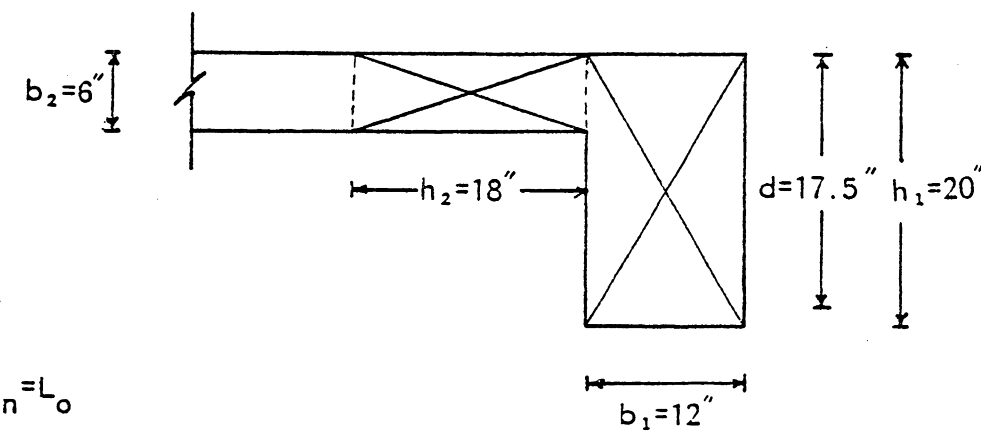

f'_c = 4000 psi

f_y = 60000 psi

L_o = 9750 lbs.

D_n = 19875 lbs.

α_t = 1.30

A_I < 400 ft², $L_n = L_o$

$V_u = 0.412(D_n + L_n)$ lbs.

$T_u = 13.60(0.736D_n + L_n)$ in-lbs.

Beam and Slab Section

Figure 5.6: Design No. 6, Source: Ref. [32]

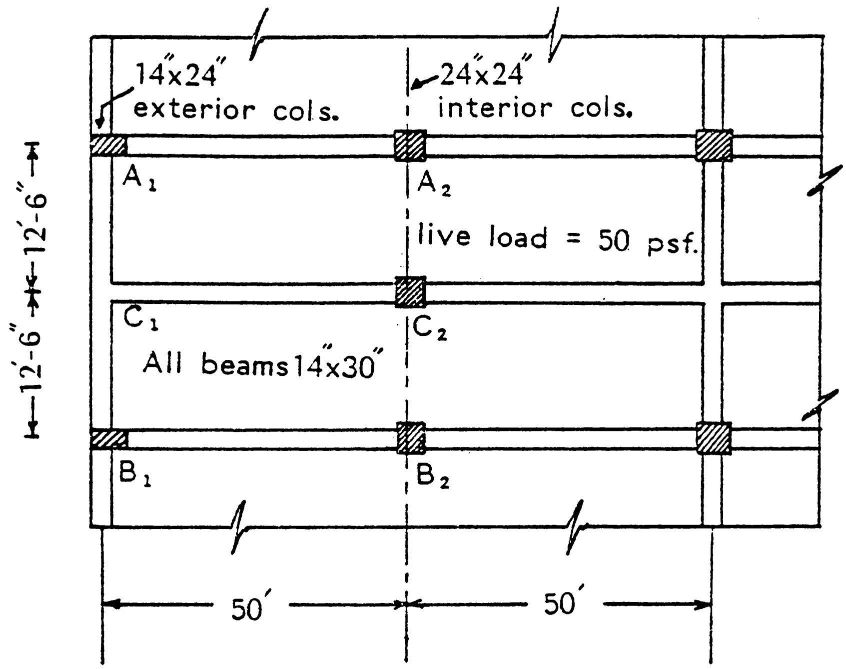

Plan

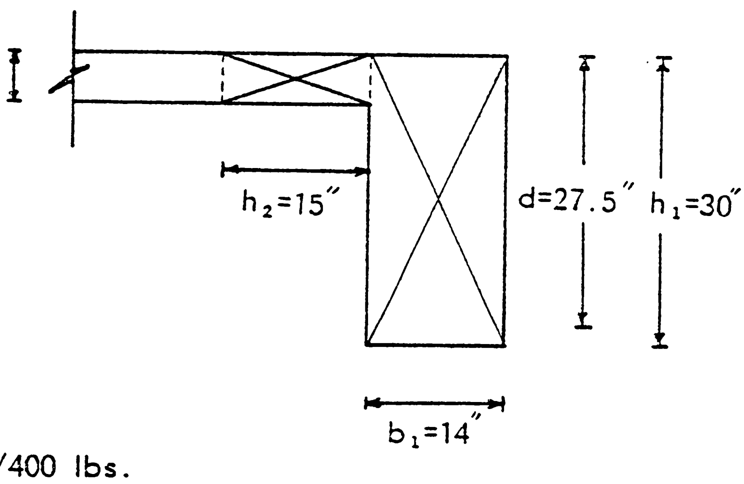

Section of Beam A_1-B_1

f'_c = 4000 psi

f_y = 60000 psi

L_o = 31250 lbs.

D_n = 57300 lbs.

α_t = 1.493

A_I = 625 ft², $L_n = 0.85 L_o$

$V_u = [75(1.392 D_n + L_n) + T_u]/400$ lbs.

$T_u = 1.134\sqrt{f'_c}(b_1^2 h_1 + b_2^2 h_2)$ in-lbs.

Figure 5.7: Design No. 7, Source: Ref. [26]

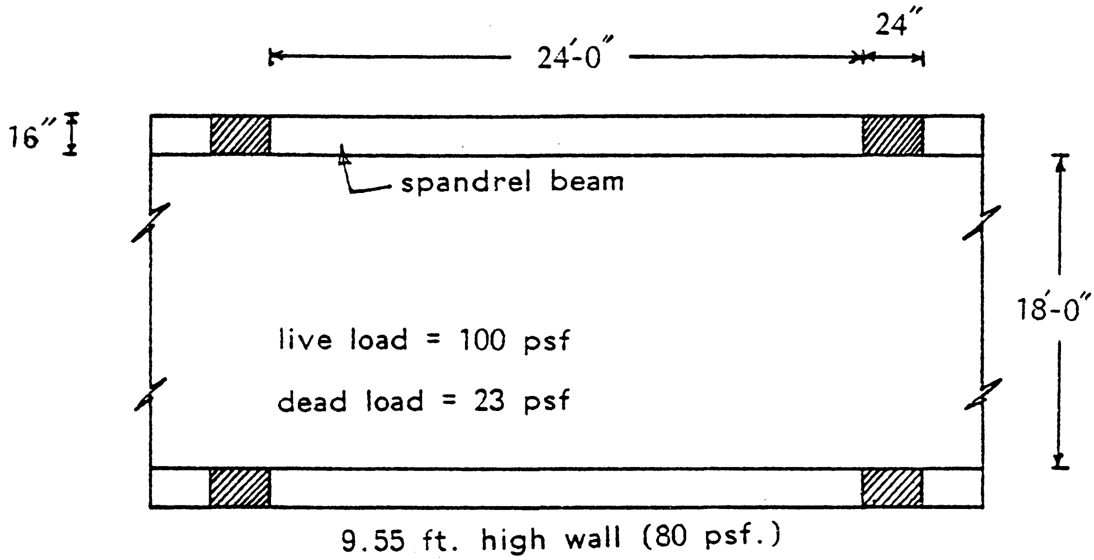

Plan

f'_c = 4000 psi
f_y = 60000 psi
L_o = 23400 lbs.
D_n = 50154 lbs.
α_t = 1.20
A_I = 468 ft², $L_n=0.943L_o$
V_u = $0.393(D_n+L_n)$ lbs.
T_u = $1.134\sqrt{f'_c}(b_1^2h_1+b_2^2h_2)$ in-lbs.

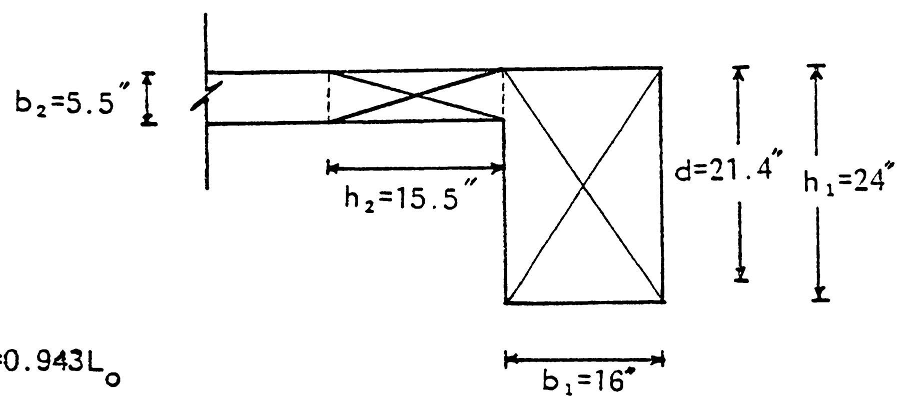

Beam and Slab Section

Figure 5.8: Design No. 8, Source: Ref. [8]

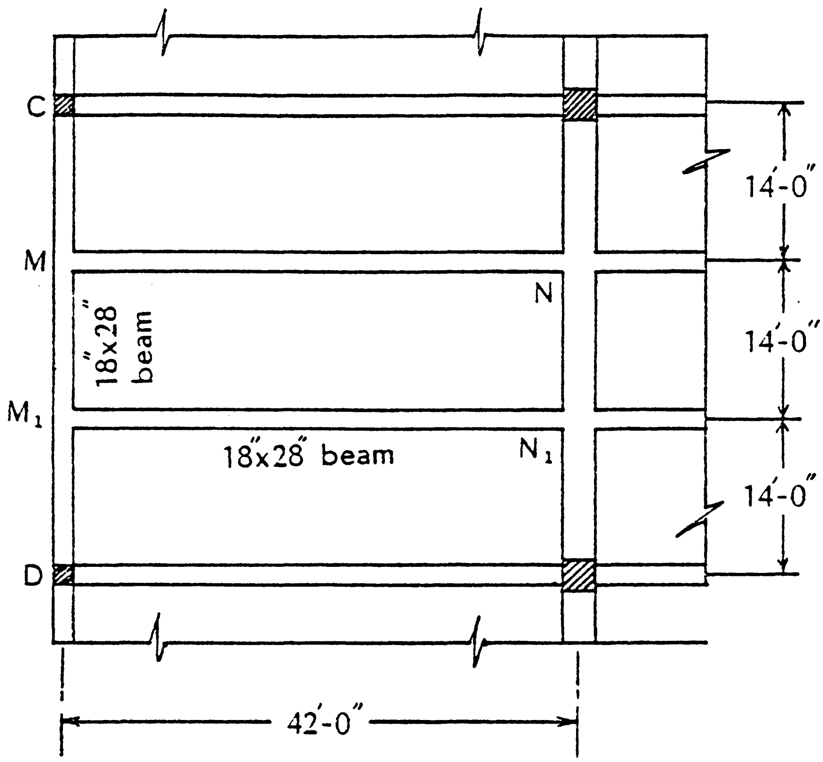

Plan

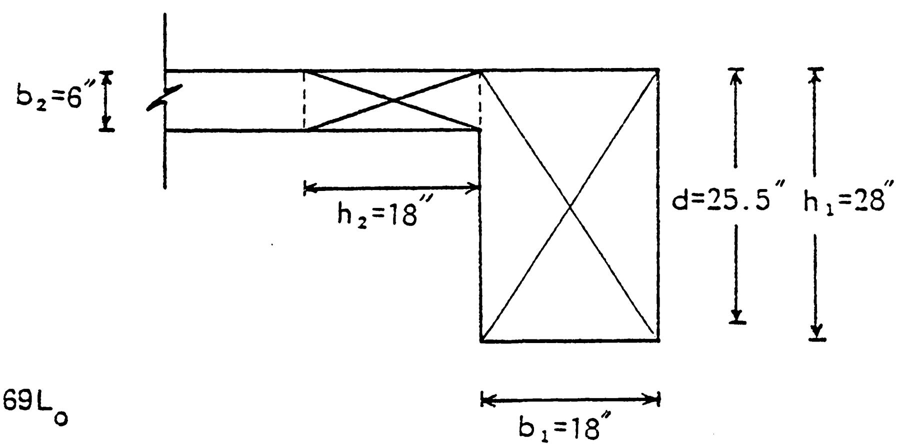

f'_c = 4000 psi
f_y = 60000 psi
L_o = 29400 lbs.
D_n = 87885 lbs.
α_t = 1.22
A_I = 1176 ft², $L_n = 0.69 L_o$
$V_u = [166.4(1.51 D_n + L_n) + T_u]/416.5$ lbs.
$T_u = 1.134\sqrt{f'_c}(b_1^2 h_1 + b_2^2 h_2)$ in-lbs.

Section of Beam C-D

Figure 5.9: Design No. 9, Source: Ref. [9]

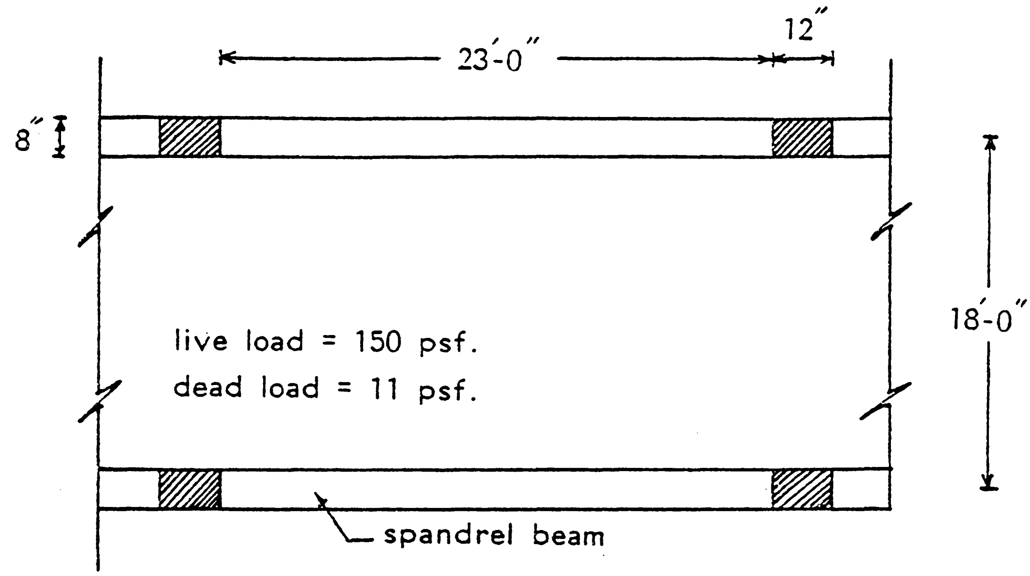

Plan

f'_c = 3000 psi

f_y = 60000 psi

L_o = 31050 lbs.

D_n = 24990 lbs.

α_t = 1.50

A_I = 432 ft², $L_n = 0.972 L_o$

$V_u = 0.422(D_n + L_n)$ lbs.

$T_u = 1.134\sqrt{f'_c}(b_1^2 h_1 + b_2^2 h_2)$ in-lbs.

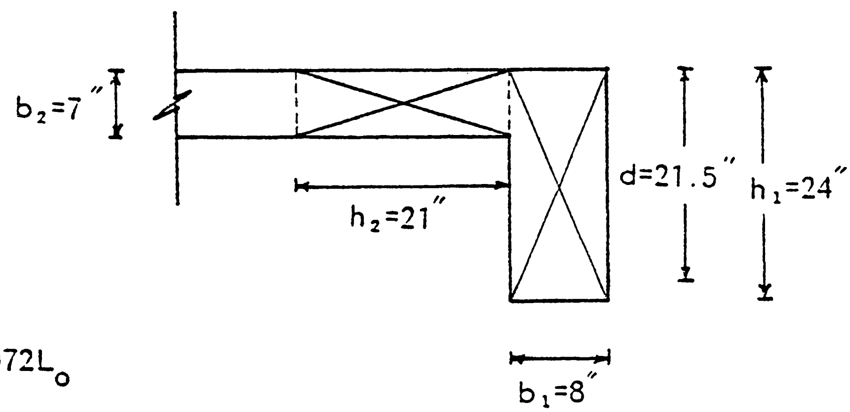

Beam and Slab Section

Figure 5.10: Design No. 10, Source: Ref. [27]

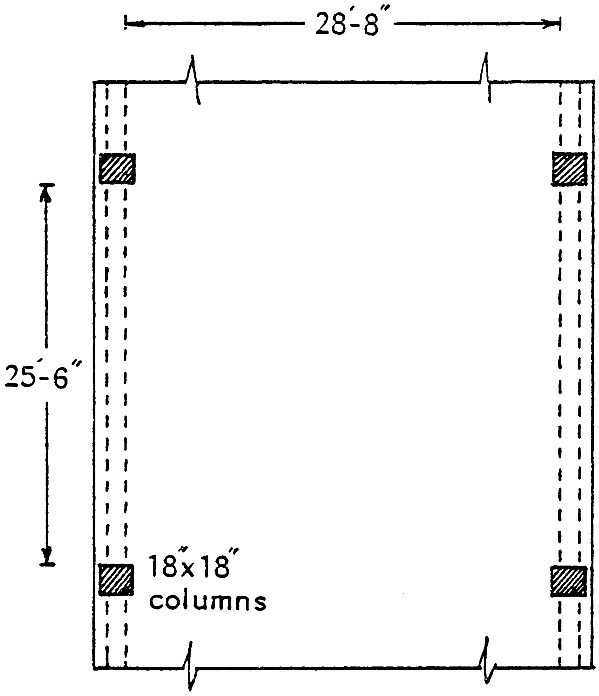

Plan

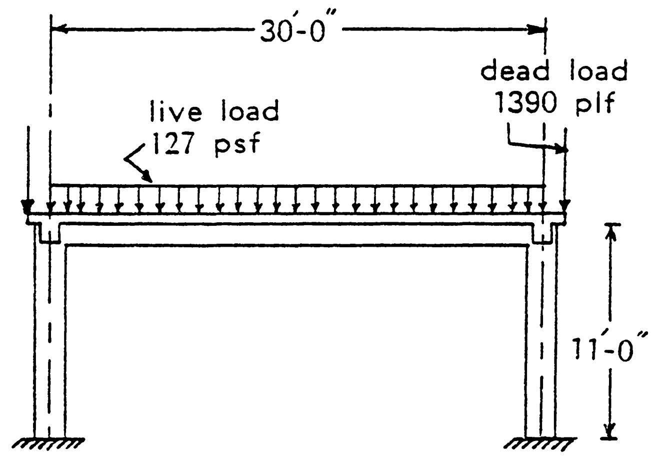

Elevation

f'_c = 4000 psi
f_y = 60000 psi
L_o = 48578 lbs.
D_n = 77775 lbs.
α_t = 1.20
A_I = 810 ft², $L_n = 0.777 L_o$
$V_u = 0.437(D_n + L_n)$ lbs.
$T_u = 1.134\sqrt{f'_c}(b_1^2 h_1 + b_2^2 h_2 + b_3^2 h_3)$ in-lbs.

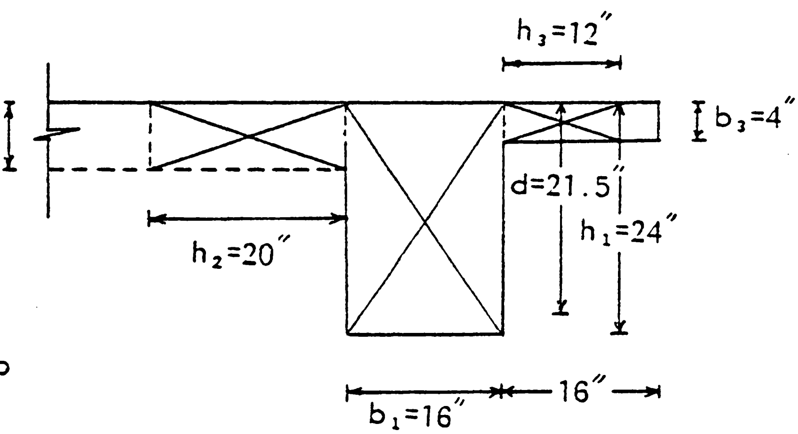

T-Beam Section

Figure 5.11: Design No. 11, Source: Ref. [22]

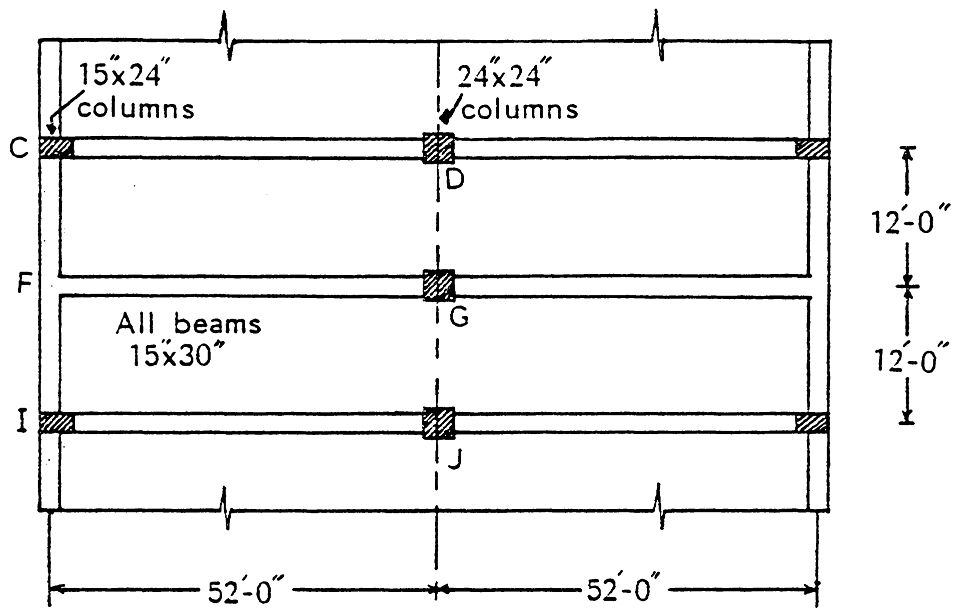

Plan

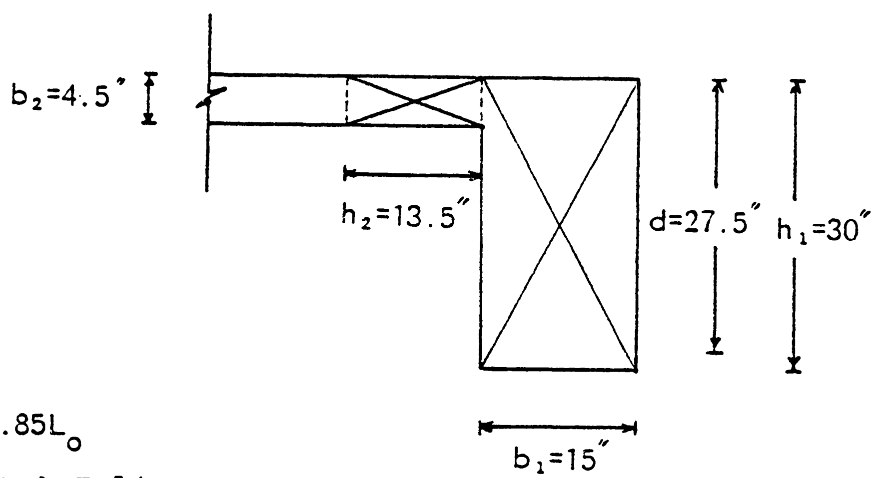

f'_c = 4000 psi

f_y = 60000 psi

L_o = 31200 lbs.

D_n = 55819 lbs.

α_t = 1.42

A_I < 624 ft², $L_n = 0.85 L_o$

$V_u = [78(1.407 D_n + L_n) + T_u]/416$ lbs.

$T_u = 1.134\sqrt{f'_c}(b_1^2 h_1 + b_2^2 h_2)$ in-lbs.

Section of Beam C-I

Figure 5.12: Design No. 12, Source: Ref. [27]

TABLE 5.1

Mean Values of Variables and Reliability Indices for Equilibrium Torsion

Design No.	1	2	3	4	5	6
Variable			Mean Value			
f'_c (psi)	4700	4700	3456	4700	4700	4700
b_1 (in.)	18	12	18	12	16	12
h_1 (in.)	28	24	27	20	32	20
b_2 (in.)	-	6	-	8	6	6
h_2 (in.)	-	18	-	24	8	18
d (in.)	25.12	21.50	24.30	17.50	29.50	17.50
x_1 (in.)	14.25	8.50	14.50	8.50	13.00	8.50
y_1 (in.)	24.25	20.50	23.50	16.50	29.00	16.50
A_t (in^2)	0.3000	0.1515	0.1045	0.1648	0.0539	0.1632
f_y (psi)	64000	64000	64000	64000	64000	64000
s (in.)	6.00	6.00	5.00	3.50	5.50	4.25
D_n (lbs.)	44100	20948	4784	23940	78855	20869
L_n (lbs.)	36000	9100	40000	5760	27000	9750
Reliability Index, β	3.10	3.36	3.11	3.15	3.65	3.22

TABLE 5.2

Mean Values of Variables and Reliability Indices for Compatibility Torsion

Design No.	7	8	9	10	11	12
Variable			Mean Value			
f'_c (psi)	4700	4700	4700	3456	4700	4700
b_1 (in.)	12	16	18	8	16	15
h_1 (in.)	30	24	28	24	24	30
b_2 (in.)	5	5.5	6	7	6.67	4.5
h_2 (in.)	15	16.5	18	21	20	13.5
b_3 (in.)	-	-	-	-	4	-
h_3 (in.)	-	-	-	-	12	-
d (in.)	27.50	21.4	25.5	21.50	21.50	27.50
x_1 (in.)	10.50	12.625	14.50	4.50	12.50	11.50
y_1 (in.)	26.50	20.625	24.50	20.50	20.50	26.50
A_t (in^2)	0.0696	0.0646	0.0900	0.0568	0.0901	0.0721
f_y (psi)	64000	64000	64000	64000	64000	64000
s (in.)	7.25	4.25	4.50	4.00	4.25	7.00
D_n (lbs.)	60165	52662	92280	26240	81664	58610
L_n (lbs.)	26563	22075	20286	30180	37745	26520
Reliability Index, β	1.88	1.99	2.09	1.88	2.05	1.90

TABLE 5.3

Variation of Reliability Index with Equilibrium Torque

Self weight of beam,

D_{n_1} = 4556 lbs.

Eccentric load = D_{n_2}

At critical section:

$V_u = 0.775D_{n_1} + D_{n_2}$ lbs.

$T_u = 10D_{n_2}$ in-lbs.

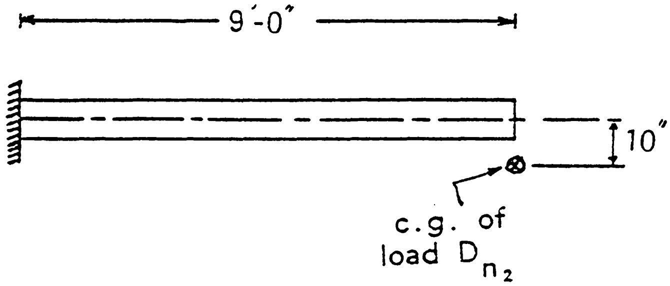

D_{n_2} (lbs.)	V_u/T_u (1/in.)	A_t/s (in²/in)	β
$5D_{n_1}$	0.1155	0.0038	3.19
$6D_{n_1}$	0.1129	0.0068	3.28
$7D_{n_1}$	0.1110	0.0097	3.22
$8D_{n_1}$	0.1097	0.0127	3.15
$9D_{n_1}$	0.1086	0.0157	3.06
$10D_{n_1}$	0.1078	0.0188	3.00
$11D_{n_1}$	0.1070	0.0218	2.92
$12D_{n_1}$	0.1065	0.0248	2.85
$13D_{n_1}$	0.1060	0.0278	2.78
$15D_{n_1}$	0.1052	0.0339	2.69
$17D_{n_1}$	0.1046	0.0400	2.62
$19D_{n_1}$	0.1041	0.0461	2.56

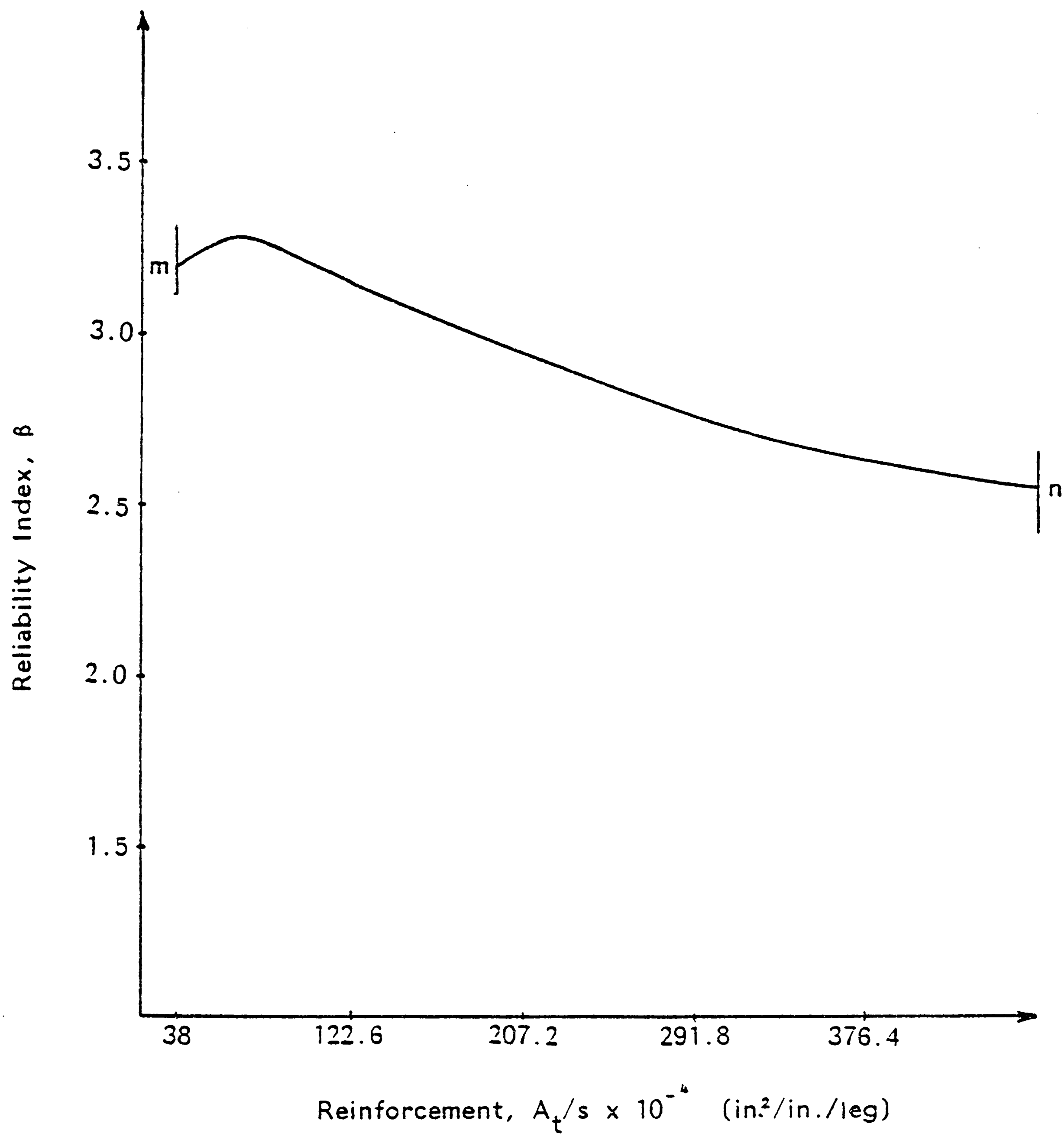

Figure 5.13: Effect of Reinforcement, A_t/s, on Reliability Index for Equilibrium Torsion

TABLE 5.4

Variation of Reliability Index with Ratio L_o/D_n for Equilibrium Torsion

Live to Dead Load Ratio L_o/D_n	Ultimate Shear to Torque Ratio V_u/T_u (1/in.)	Reinforcement A_t/s (in²/in.)	Reliability Index β
0.00	0.1100	0.0121	3.16
0.25	0.1095	0.0132	3.49
0.50	0.1093	0.0139	3.54
0.75	0.1090	0.0145	3.54
1.00	0.1089	0.0149	3.50
1.25	0.1088	0.0152	3.46
1.50	0.1087	0.0155	3.43
1.75	0.1086	0.0157	3.40
2.00	0.1086	0.0158	3.36

Total Load (L_o+D_n) = 40,000 lbs.
$L_n = L_o$

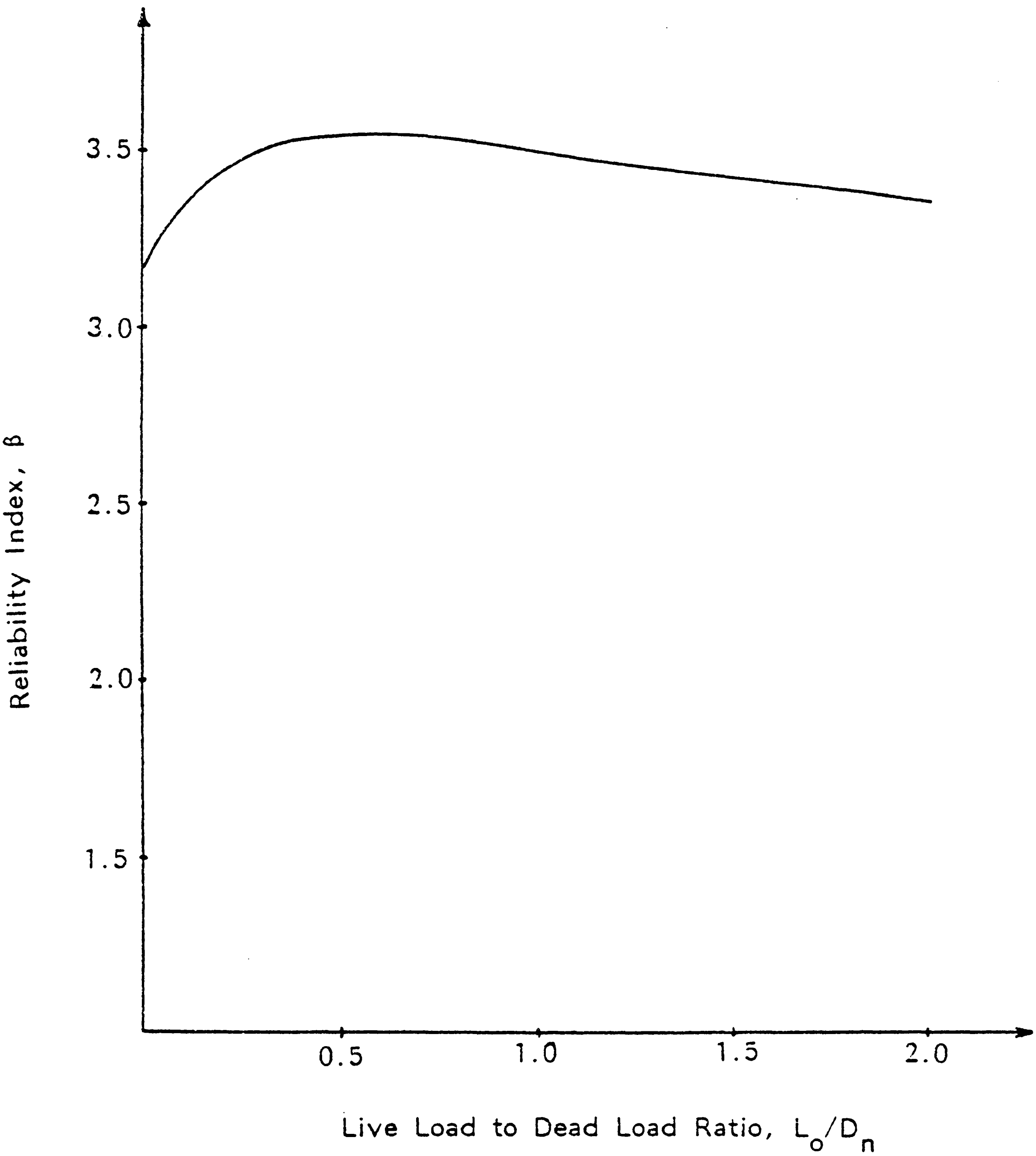

Figure 5.14: Effect of Ratio L_o/D_n on Reliability Index for Equilibrium Torsion

TABLE 5.5

Variation of Reliability Index with Compatibility Torque

Self weight of beam and slab,

D_{n_1} = 42350 lbs.

Superimposed load = D_{n_2}

At critical section:

$V_u = 0.437(D_{n_1}+D_{n_2})$ lbs.

$T_u = 1.134\sqrt{f'_c}(\Sigma b^2h)$ in-lbs.

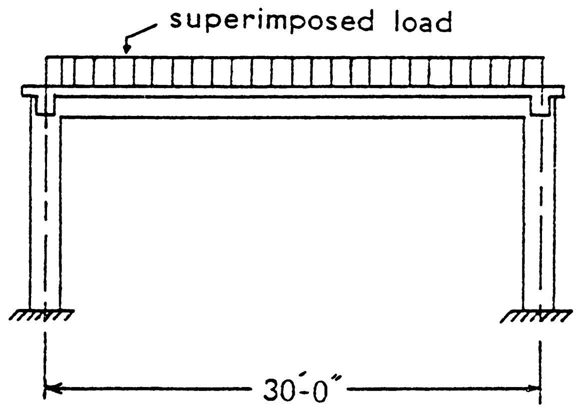

D_{n_2} (lbs.)	V_u/T_u (1/in.)	A_t/s (in²/in)	β
0	0.050	0.0148	1.87
$0.5D_{n_1}$	0.075	0.0163	1.91
$1.0D_{n_1}$	0.100	0.0179	1.90
$1.5D_{n_1}$	0.125	0.0194	1.85
$2.0D_{n_1}$	0.150	0.0207	1.76
$2.5D_{n_1}$	0.175	0.0219	1.69
$3.0D_{n_1}$	0.200	0.0229	1.60
$3.5D_{n_1}$	0.225	0.0238	1.53
$4.0D_{n_1}$	0.250	0.0245	1.45
$4.5D_{n_1}$	0.275	0.0252	1.39
$5.0D_{n_1}$	0.300	0.0257	1.33
$5.5D_{n_1}$	0.325	0.0262	1.28

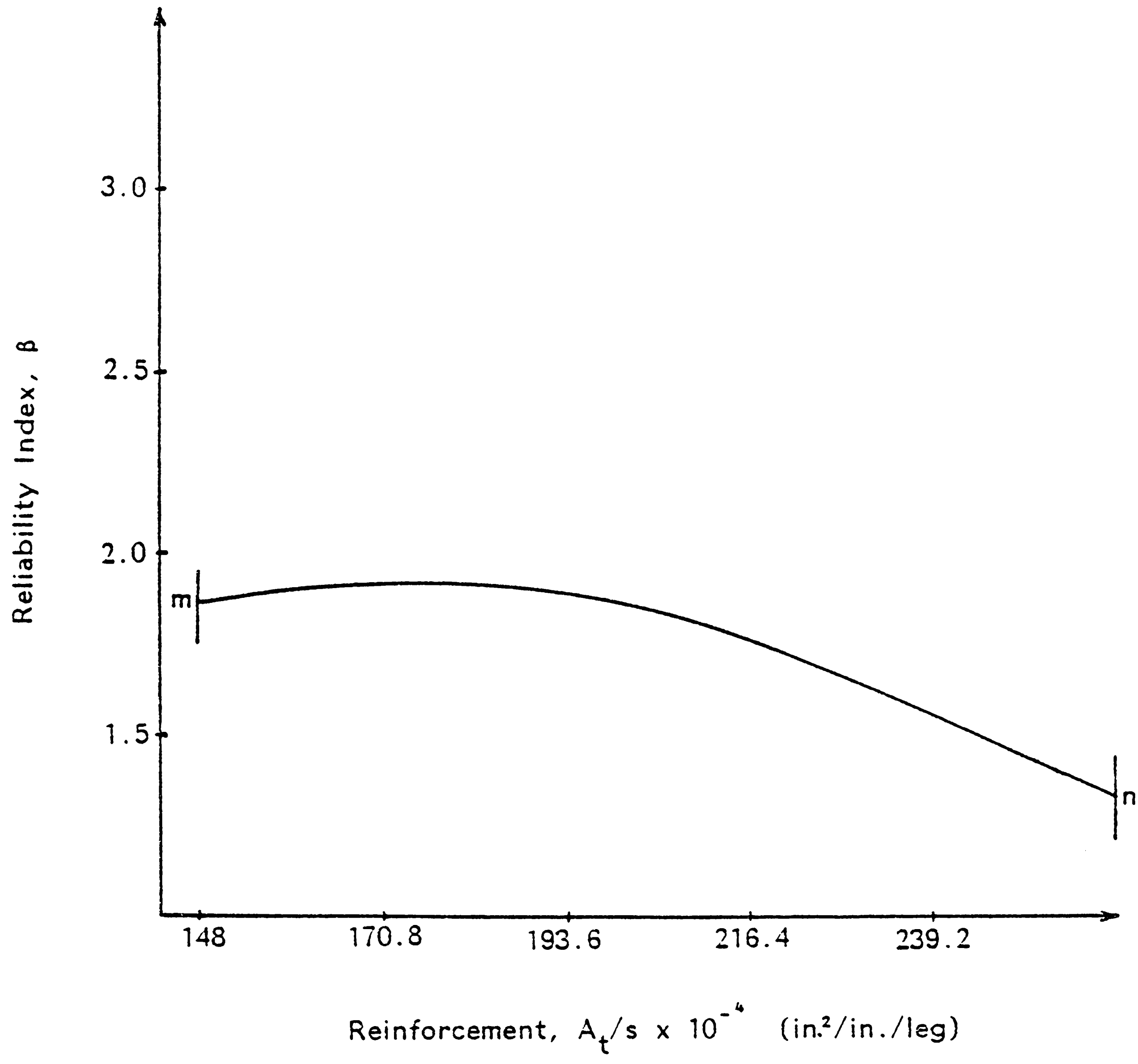

Figure 5.15: Effect of Reinforcement, A_t/s, on Reliability Index for Compatibility Torsion

TABLE 5.6

Variation of Reliability Index with Ratio L_o/D_n for Compatibility Torsion

Live to Dead Load Ratio L_o/D_n	Ultimate Shear to Torque Ratio V_u/T_u (1/in.)	Reinforcement A_t/s (in²/in.)	Reliability Index β
0.00	0.1500	0.0207	1.76
0.25	0.1565	0.0210	1.92
0.50	0.1608	0.0212	2.02
0.75	0.1639	0.0214	2.10
1.00	0.1662	0.0215	2.14
1.25	0.1679	0.0216	2.18
1.50	0.1694	0.0216	2.18
1.75	0.1705	0.0217	2.23
2.00	0.1715	0.0217	2.24

Total Load (L_o+D_n) = 127,050 lbs.
$L_n = 0.777L_o$

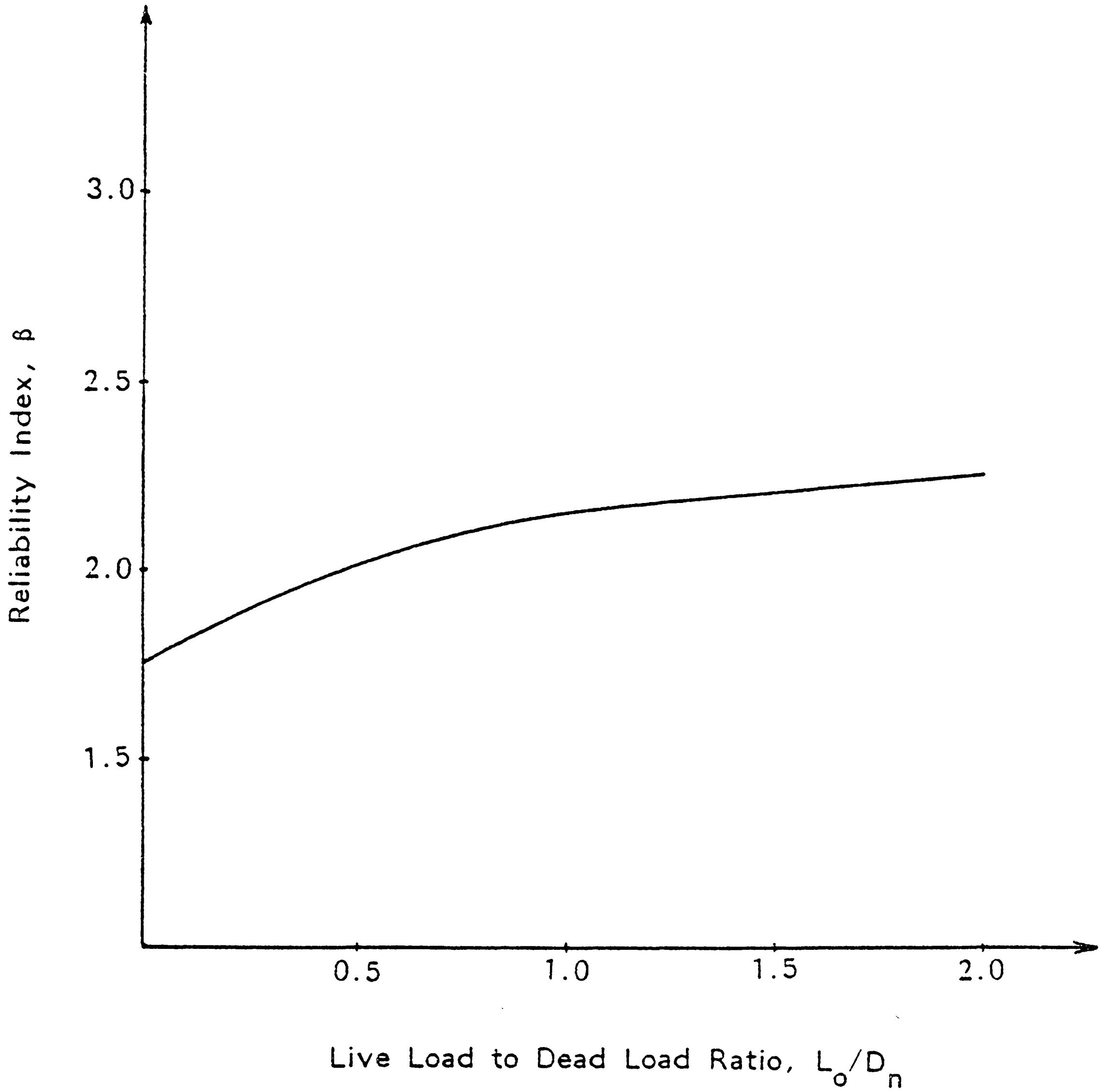

Figure 5.16: Effect of Ratio L_o/D_n on Reliability Index for Compatibility Torsion

Chapter VI

SUMMARY AND CONCLUSIONS

6.1 SUMMARY

Current ACI code requirements for the design of torsional reinforced concrete members have been summarized and reliability analysis was used to determine the risk, or conversely the level of safety, implied in these code provisions. Risk levels for a number of reinforced concrete beams, subjected to equilibrium and compatibility torsion and designed in accordance with ACI code provisions, were computed. The effect of applied torque, T_u, and basic live load to nominal dead load ratio, L_o/D_n, on the reliability of reinforced concrete beams subjected to torsion was also investigated.

Advanced first-order, second-moment analysis was used as a basis for the computation of the reliability index, β. In this method, the limit state equation is linearized at discreet points on the failure surface. The statistical data used for the evaluation of uncertainties was obtained from available studies.

Reliability indices were computed separately for beams designed to carry equilibrium torque and for beams subjected to compatibility torsion. The effect of torsional loading and ratio L_o/D_n on the reliability index was compared for the two types of torsion.

5.2 CONCLUSIONS

Following conclusions can be drawn from the results of this study:

1. Risk levels for reinforced concrete members in torsion are comparable to those obtained for reinforced concrete members subjected to flexure and shear.
2. It was found that reliability indices for equilibrium torsion were higher than those for compatibility torsion. For the beam designs considered in this study, the reliability index for equilibrium torsion ranged from 3.10 to 3.65 while the reliability index for compatibility torsion ranged from 1.88 to 2.09.
3. For both equilibrium and compatibility torsion, the reliability index decreases as the reinforcement A_t/s is increased.
4. In the case of compatibility torsion, the increase in torsional loading has a less pronounced effect on the reliability index, as compared to the case of equilibrium torsion. This is due to the ACI provision (Eq. 2.12) for moment redistribution, in which the design torque is a function of concrete strength and member dimensions instead of applied loading.
5. The reliability index increases with an increase in L_o/D_n ratio (Fig. 5.16), when a reduction is allowed in the basic live load for influence areas greater than 400 ft^2. If the basic live load is not reduced, then the effect of ratio L_o/D_n on reliability index is the same as that for the increase in reinforcement A_t/s.

6. The variation in the in the reliability index with torsional loading and ratio L_o/D_n is a function of ratio V_u/T_u, for both equilibrium and compatibility torsion.

REFERENCES

1. Ang, A. H-S., "Structural Risk Analysis and Reliability-Based Design," Journal of the Structural Division, ASCE, Vol. 99, No. ST9, September, 1973, pp. 1891-1910.

2. Ang, A. H-S. and Amin, M., "Safety Factors and Probability in Structural Design," Journal of the Structural Division, ASCE, Vol. 95, No. ST7, July, 1969, pp. 1389-1405.

3. Ang, A. H-S. and Cornell, C.A., "Reliability Bases of Structural Safety and Design," Journal of the Structural Division, ASCE, Vol. 100, No. ST9, September, 1974, pp. 1755-1769.

4. Ang, A. H-S. and Tang, W.H., Probability Concepts in Engineering Planning and Design, Vol. II, John Wiley, New York, 1984.

5. "Building Code Requirements for Reinforced Concrete (ACI 318-83)," American Concrete Institute, Detroit, 1983.

6. Cornell, C.A., "A Probability Based Structural Code," American Concrete Institute Journal, December, 1969, pp. 974-985.

7. Costello, J.F. and Chu, K., "Failure Probabilities of Reinforced Concrete Beams," Journal of the Strucural Division, ASCE, Vol. 95, No. ST10, October, 1969, pp. 2281-2304.

8. "CRSI Handbook," Concrete Reinforcing Steel Institute, 3rd edition, Skokie, 1978, pp. 12-38 to 12-43.

9. "Design of Concrete Beams for Torsion," PCA Design Aid (EB106.01D), Portland Cement Association, Skokie, 1983.

10. Ellingwood, B.R., "Reliability of Current Reinforced Concrete Designs," Journal of the Structural Division, ASCE, Vol. 105, No. ST4, April, 1979, pp. 699-712.

11. Ellingwood, B.R., "Reliability Based Criteria for Reinforced Concrete Design," Journal of the Structural Division, ASCE, Vol. 105, No. ST4, April, 1979, pp. 713-727.

12. Ellingwood, B.R., "Safety Checking Formats for Limit States Design," Journal of the Structural Division, ASCE, Vol. 108, No. ST7, July, 1982, pp. 1481-1493.

13. Ellingwood, B.R. and Ang, A. H-S., "Risk-Based Evaluation of Design Criteria," Journal of the Structural Division, ASCE, Vol. 100, No. ST9, September, 1974, pp. 1771-1788.

14. Ellingwood, B.R., MacGregor, J.G., Galambos, T.V., and Cornell, C.A., "Probability Based Load Criteria: Load Factors and Load Combinations," Journal of the Structural Division, ASCE, Vol. 108, No. ST5, May, 1982, pp. 978-997.

15. Ferguson, P.H., Reinforced Concrete Fundamentals, John Wiley, 4th edition, 1979, pp. 160-162.

16. Freudenthal, A.M., "The Safety of Structures," Transactions, ASCE, Vol. 112, 1947, pp. 125-180.

17. Freudenthal, A.M., "Safety and the Probability of Structural Failure," Transactions, ASCE, Vol. 121, 1956, pp. 1337-1375.

18. Freudenthal, A.M., "Safety, Reliability and Structural Design," Journal of the Structural Division, ASCE, Vol. 87, No. ST3, March, 1961, pp. 1-16.

19. Freudenthal, A.M., Garrelts, J.M., and Shinozuka, M., "The Analysis of Structural Safety," Journal of the Structural Division, ASCE, Vol. 92, No. ST1, February, 1966, pp. 267-325.

20. Galambos, T.V., Ellingwood, B.R., MacGregor, J.G., and Cornell, C.A., "Probability Based Load Criteria: Assessment of Current Design Practice," Journal of the Structural Division, ASCE, Vol. 108, No. ST5, May, 1982, pp. 959-977.

21. Hasofer, A.M. and Lind, N.C., "Exact and Invariant Second-Moment Code Format," Journal of the Engineering Mechanics Division, ASCE, Vol. 100, No. EM1, February, 1974, pp. 111-121.

22. Hsu, T.T.C., Torsion of Reinforced Concrete, Van Nostrand Reinhold, New York, 1984.

23. Lind, N.C., "Consistent Partial Safety Factors," Journal of the Structural Division, ASCE, Vol. 97, No. ST6, June, 1971, pp. 1651-1669.

24. Mirza, S.A. and MacGregor, J.G., "Variability of Mechanical Properties of Reinforcing Bars," Journal of the Structural Division, ASCE, Vol. 105, No. ST5, May, 1979, pp. 921-937.

25. "National Bureau of Standards Special Publication No. 577," National Bureau of Standards, Washington, June, 1980.

26. Nawy, E.G., Reinforced Concrete-A fundamental approach, Prentice Hall, 1985, pp. 226-241.

27. "Notes on ACI 318-77 Building Code Requirements for Reinforced Concrete," Portland Cement Association, 3rd edition, Skokie, 1980, pp. 14-1 to 14-33.

28. Pugsley, A.G., The Safety of Structures, Edward Arnold Publishers, 1st edition, London, 1966.

29. Ravindra, M.K., Lind, N.C., and Siu, W.W.C., "Illustrations of Reliability-Based Design," Journal of the Structural Division, ASCE, Vol. 100, No. ST9, September, 1974, pp. 1789-1811.

30. Siu, W.W.C., Parimi, S.R., and Lind, N.C., "Practical Approach to Code Calibration," Journal of the Structural Division, ASCE, Vol. 101, No. ST7, July, 1975, pp. 1469-1480.

31. Surahman, A. and Rojiani, K.B., "Reliability Based Optimum Design of Concrete Frames," Journal of the Structural Division, ASCE, Vol. 109, No. ST3, March, 1983, pp. 741-757.

32. "Torsion of Structural Concrete," Special Publication SP-18, American Concrete Institute, Detroit, 1968, pp. 483-491.

33. Winter, G. and Nilson, A.H., Design of Concrete Structures, John Wiley, 9th ed., New York, 1979.

Appendix A

CALCULATION DETAILS

A.1 CALCULATION DETAILS OF DESIGN NO. 1

Superimposed loads:

Nominal dead load, D_n = 42000 lbs.

Nominal live load, L_n = 36000 lbs.

Self weight of beam,

$$W_d = \frac{18(28)}{144} \times 150 \text{ plf.} \times 30 \text{ ft.} = 15{,}750 \text{ lbs.}$$

or

$$W_d = \frac{15750}{42000} D_n = 0.375\ D_n$$

Shear at distance 'd' from column face [Fig. A-1]:

$$V_u = \frac{D_n+L_n}{2} + \frac{15-2.09}{15} \times \frac{W_d}{2}$$

$$= 0.5(D_n+L_n) + 0.43W_d$$

Substituting $W_d = 0.375\ D_n$, the critical shear becomes,

$$V_u = 0.5(D_n+L_n) + 0.43(0.375D_n)$$

$$= 0.5(1.323D_n+L_n)$$

Applied torque will be constant throughout the beam and its value is:

$$T_u = \frac{\text{torsional load} \times \text{moment arm}}{2}$$

$$= \frac{(D_n+L_n)}{2} \text{ lbs.} \times 24 \text{ in.} = 12(D_n+L_n) \text{ in-lbs.}$$

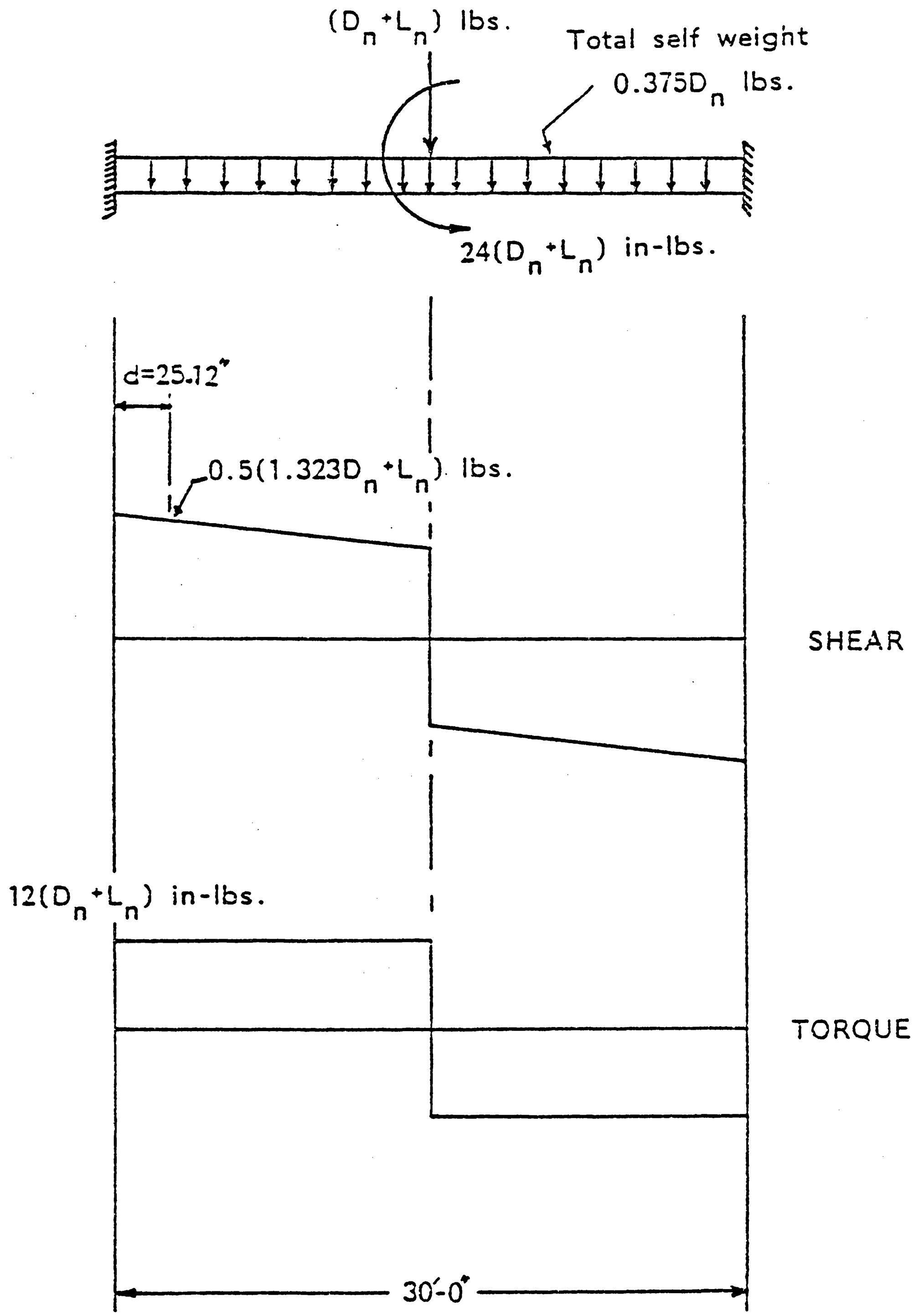

Figure A-1: Shear and Torque Diagrams for Design No. 1

$$\frac{V_u}{T_u} = \frac{0.5(1.323D_n+L_n)}{12(D_n+L_n)} = \frac{1.323D_n+L_n}{24(D_n+L_n)}$$

The performance function is:

$$G = T_c + T_s - T_u$$

where

$$T_c = \frac{0.8\sqrt{f'_c}(\Sigma b^2h)}{\sqrt{1+\left[\dfrac{0.4(\Sigma b^2h)V_u}{b_w d T_u}\right]^2}}$$

and

$$T_s = \alpha_t x_1 y_1 A_t f_y/s$$

For a rectangular beam, $\Sigma b^2h=b^2h$ and $b_w=b$. Rearranging T_c,

$$T_c = \frac{0.8\sqrt{f'_c}}{\left[\dfrac{1}{b^2h} + \dfrac{0.16V_u^2}{b^2d^2T_u^2}\right]^{1/2}}$$

Substituting the values of V_u, T_u and α_t in the performance function,

$$G = \frac{0.8\sqrt{f'_c}}{\left[\dfrac{1}{b^4h^2} + \dfrac{(1.323D_n+L_n)^2}{3600b^2d^2(D_n+L_n)^2}\right]^{1/2}} + 1.22x_1y_1A_tf_y/s - 12(D_n+L_n)$$

Let $N = \dfrac{1.323D_n + L_n}{D_n + L_n}$

and $DENOM = \dfrac{1}{b^4 h^2} + \dfrac{N^2}{3600 b^2 d^2}$

Then the partial deratives with respect to the basic variables in the performance function are as follows:

$$\frac{\partial G}{\partial f_c} = \frac{0.4}{[f'_c(DENOM)]^{1/2}}$$

$$\frac{\partial G}{\partial b} = \frac{1.6\sqrt{f'_c}}{(DENOM)^{3/2}} \left[\frac{1}{b^5 h^2} + \frac{N^2}{7200 b^3 d^2} \right]$$

$$\frac{\partial G}{\partial h} = \frac{0.8\sqrt{f'_c}}{b^4 h^3 (DENOM)^{3/2}}$$

$$\frac{\partial G}{\partial d} = \frac{\sqrt{f'_c}\ N^2}{4500 b^2 d^3 (DENOM)^{3/2}}$$

$$\frac{\partial G}{\partial x_1} = 1.22 y_1 A_t f_y / s$$

$$\frac{\partial G}{\partial y_1} = 1.22 x_1 A_t f_y / s$$

$$\frac{\partial G}{\partial A_t} = 1.22 x_1 y_1 f_y / s$$

$$\frac{\partial G}{\partial f_y} = 1.22 x_1 y_1 A_t / s$$

$$\frac{\partial G}{\partial s} = -1.22 x_1 y_1 A_t f_y / s^2$$

$$\frac{\partial G}{\partial D_n} = - \frac{\sqrt{f'_c}\, L_n (1.323 D_n + L_n)}{13932 b^2 d^2 (D_n + L_n)^3 (DENOM)^{3/2}} - 12$$

$$\frac{\partial G}{\partial L_n} = - \frac{\sqrt{f'_c}\, D_n (1.323 D_n + L_n)}{13932 b^2 d^2 (D_n + L_n)^3 (DENOM)^{3/2}} - 12$$

The iteration results are presented in Table A-1.

A.2 <u>CALCULATION DETAILS OF DESIGN NO. 7</u>

Nominal service dead load of beam C_1-C_2,

$$D_n = \frac{5.0}{12} \times 12.5 + \frac{25 \times 14}{144}\ 150 \text{ plf.} \times 50 \text{ ft.}$$

$$= 1146 \text{ plf.} \times 50 \text{ ft.} = 57{,}300 \text{ lbs.}$$

Basic service live load of beam C_1-C_2,

$$L_o = (50 \times 12.5) \text{ plf.} \times 50 \text{ ft.} = 31{,}250 \text{ lbs.}$$

Nominal live load of beam C_1-C_2,

$$L_n = 0.85 L_o = 26563 \text{ lbs.}$$

Fixed end moment,

$$FEM = \frac{W_u L}{12} = \frac{(D_n + L_n) \times 50}{12} \text{ ft-lbs.} = 50(D_n + L_n) \text{ in-lbs.}$$

TABLE A.1

Results for Design No. 1

Initial β = 3.00

Cycle No.	Variable	Initial x_i^*	$\partial G/\partial x_i^*$	α_i^*	New x_i^*
	f_c	4700	49863	0.2063	4089.2
	b	18.00	35556	0.1471	17.64
	h	28.00	16411	0.0679	27.74
	d	25.12	4472	0.0185	25.00
	x_1	14.25	69827	0.2889	13.19
1	y_1	24.25	69827	0.2889	22.44
	A_t	0.300	27385	0.1133	0.2963
	f_y	64000	160783	0.6651	44844
	s	6.00	-60692	-0.2511	6.39
	D_n	44100	-53258	-0.2203	47015
	L_n	36000	-107325	-0.4440	47988
β = 3.1006					
	f_c	4089	49937	0.2080	4064
	b	17.64	35418	0.1475	17.63
	h	27.74	16343	0.0681	27.73
	d	25.00	4440	0.0185	25.00
	x_1	13.19	68562	0.2885	13.17
2	y_1	22.44	68562	0.2885	22.40
	A_t	0.2963	26850	0.1118	0.2963
	f_y	44844	160019	0.6664	44163
	s	6.39	-59426	-0.2475	6.40
	D_n	47015	-53255	-0.2218	47133
	L_n	47988	-107336	-0.4470	48474
β = 3.1005					

The moment distribution is shown in Fig. A-2(a). From Fig. A-2(b), the reaction at point C_1, which is also the middle point of spandrel beam A_1-B_1, can be calculated as follows:

$$R_{C_1} = \frac{2T_u + 300(D_n+L_n) + 75(D_n+L_n) - T_u}{600}$$

Self weight of beam A_1-B_1,

$$W_d = \frac{14 \times 30}{144} \times 150 \text{ plf.} \times 25 \text{ ft.} = 10938 \text{ lbs.}$$

or

$$W_d = \frac{10938}{57300} D_n = 0.191 D_n$$

Critical section is at a distance d=2.88 ft. from column face. Therefore, critical shear can be computed as [Fig. A-3]:

$$V_u = \frac{R_{C_1}}{2} + \frac{12.5 - 2.88}{12.5} W_d \quad \text{lbs.}$$

Substituting the values of R_{C_1} and W_d,

$$V_u = \frac{75(D_n+L_n) + T_u}{400} + 0.385(0.191 D_n)$$

$$= \frac{75(1.392D_n+L_n) + T_u}{400} \quad \text{lbs.}$$

From Eq. 2.14, the ultimate value of torque to be used is

$$T_u = 0.85[4\sqrt{f'_c}(\Sigma b^2 h/3)] \text{ in-lbs.}$$

Therefore,

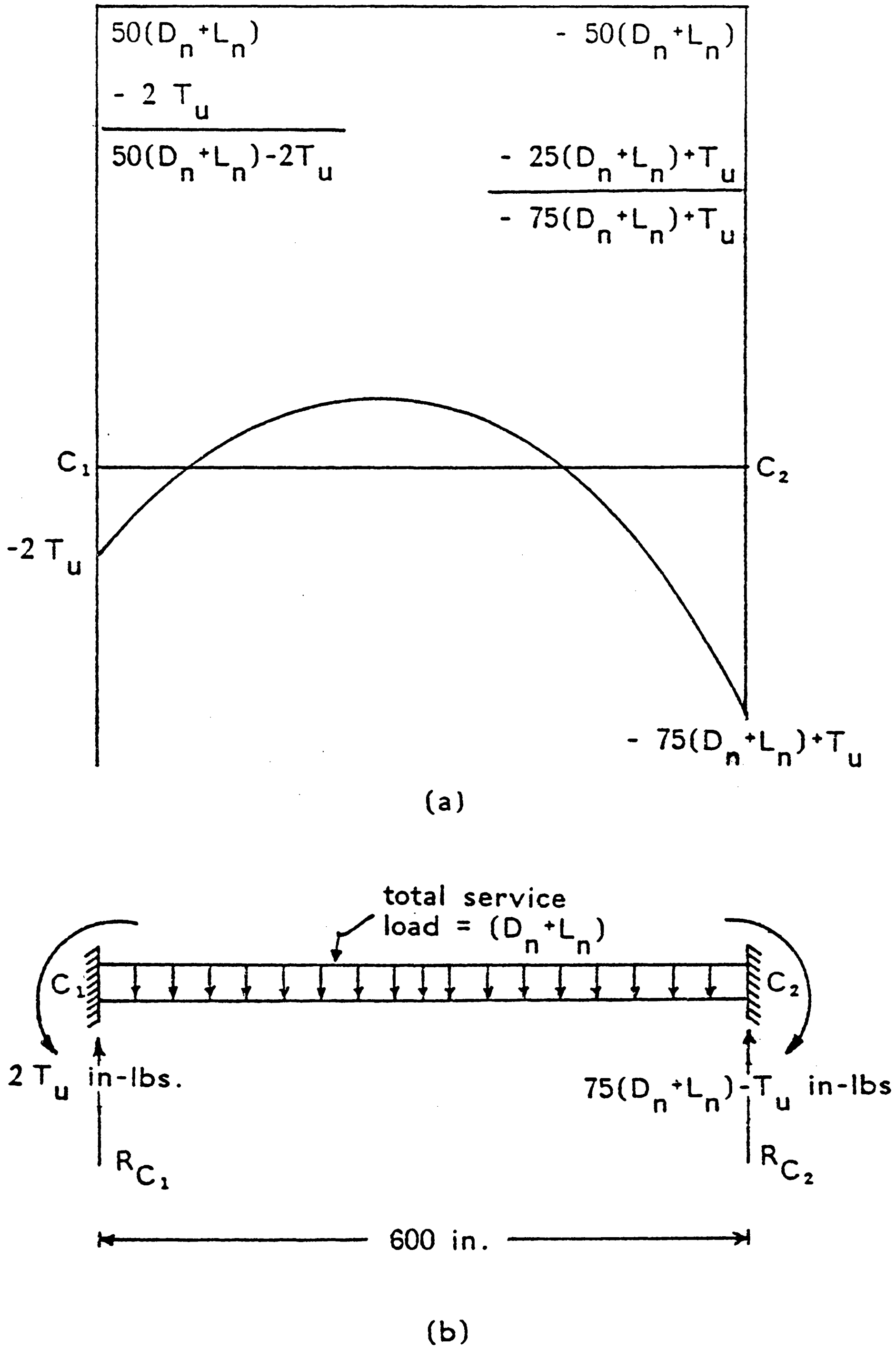

Figure A.2: Moment Distribution for Design No. 7

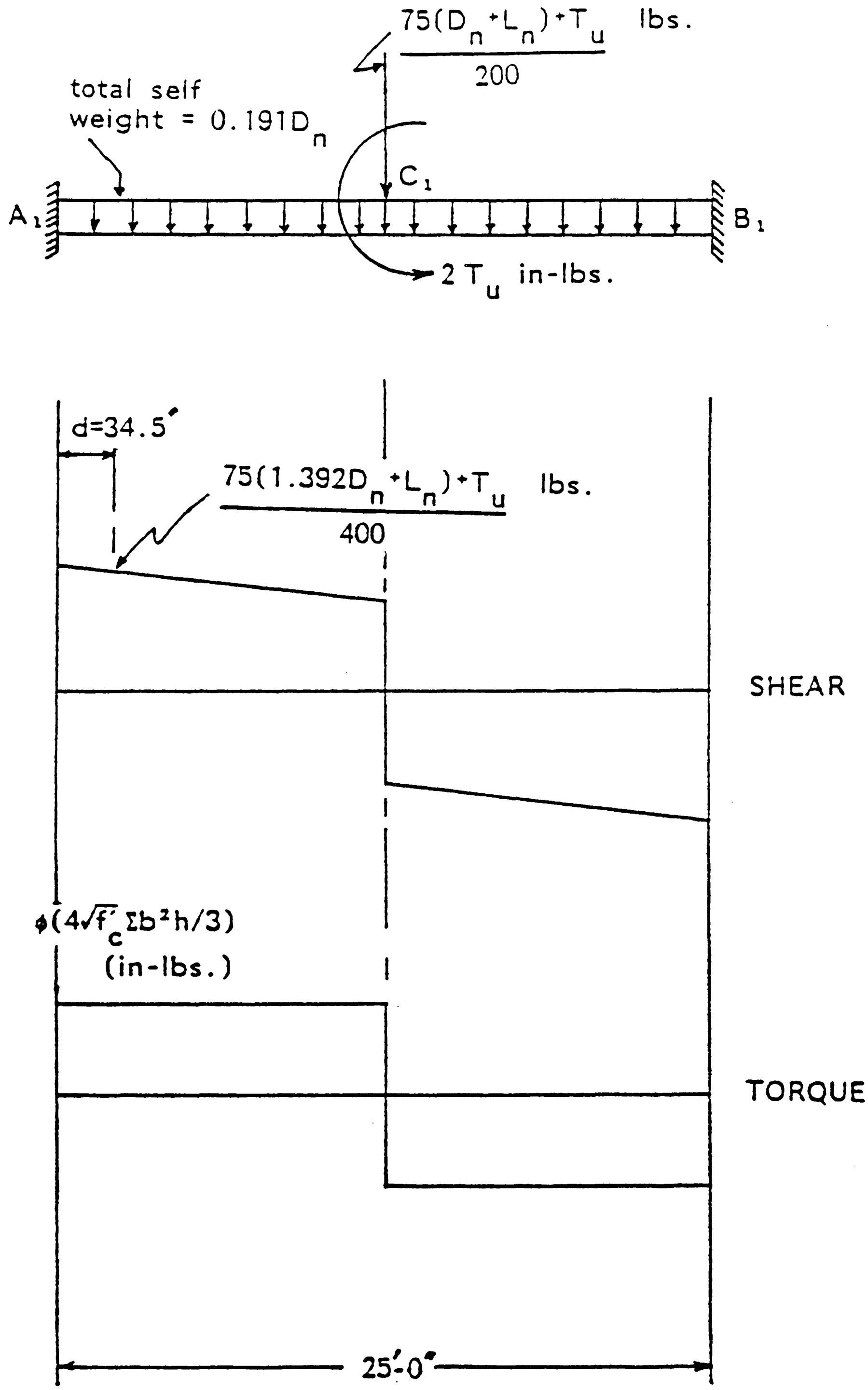

Figure A-3: Shear and Torque Diagrams for Design No. 7

$$\frac{V_u}{T_u} = \frac{75(1.392D_n + L_n)}{400 \times 0.85 \times 4\sqrt{f'_c}(\Sigma b^2 h/3)} + \frac{1}{400}$$

$$= \frac{(1.392D_n + L_n)}{6.04\sqrt{f'_c}(\Sigma b^2 h)} + \frac{1}{400}$$

The performance function is:

$$G = T_c + T_s - T_u$$

where

$$T_c = \frac{0.8\sqrt{f'_c}(\Sigma b^2 h)}{\sqrt{1 + \left[\frac{0.4(\Sigma b^2 h)V_u}{b_w d T_u}\right]^2}}$$

and

$$T_s = \alpha_t x_1 y_1 A_t f_y / s$$

For an L-beam, $\Sigma b^2 h = b_1^2 h_1 + b_2^2 h_2$, and $b_w = b_1$. Rearranging T_c,

$$T_c = \frac{1}{\left[\frac{1}{0.64 f'_c (\Sigma b^2 h)^2} + \frac{0.16 V_u^2}{0.64 f_c b_1^2 d^2 T_u^2}\right]^{1/2}}$$

Substituting the value of V_u/T_u in the above expression and rearranging,

$$T_c = \frac{1}{\left\{\left[\frac{1}{0.64f'_c(b_1^2h_1+b_2^2h_2)^2} + \frac{1}{d^2}\left[\frac{(1.392D_n+L_n)}{12.1f'_c(b_1^3h_1+b_1b_2^2h_2)} + \frac{1}{800\sqrt{f'_c}b_1}\right]^2\right]\right\}^{1/2}}$$

Let $N_1 = 1.392D_n+L_n$

$$N_2 = b_1^2h_1 + b_2^2h_2$$

$$N_3 = b_1^3h_1 + b_1b_2^2h_2$$

$$N_4 = \frac{N_1}{12.1\ f'_c\ N_3} + \frac{1}{800\sqrt{f'_c}b_1}$$

$$\text{DENOM} = \frac{1}{0.64f'_c(N_2)^2} + \frac{(N_4)^2}{d^2}$$

The performance function can be written as:

$$G = \frac{1}{\left[\frac{1}{0.64\ \sqrt{f'_c}(N_2)^2} + \frac{(N_4)^2}{d^2}\right]^{1/2}} + 1.493x_1y_1A_tf_y/s - 1.134\sqrt{f'_c}N_2$$

The partial derivatives with respect to the basic variables in the performance function are as follows:

$$\frac{\partial G}{\partial f'_c} = \frac{1}{(\text{DENOM})^{3/2}}\left\{\frac{1}{1.28(f'_c)^2(N_2)^2} + \frac{N_4}{d^2}\left[\frac{N_1}{12.1(f'_c)^2N_3} + \frac{1}{1600(f'_c)^{3/2}b_1}\right]\right\} - \frac{0.567N_2}{\sqrt{f'_c}}$$

$$\frac{\partial G}{\partial b_1} = \frac{1}{(DENOM)^{3/2}} \left\{ \frac{b_1 h_1}{0.32\ f'_c (N_2)^3} + \frac{N_4}{d^2} \left[\frac{N_1 (3b_1^2 h_1 + b_2^2 h_2)}{12.1\ f'_c (N_3)^2} + \frac{1}{800\sqrt{f'_c}\, b_1^2} \right] \right\} - 2.268\sqrt{f'_c}\, b_1 h_1$$

$$\frac{\partial G}{\partial h_1} = \frac{1}{(DENOM)^{3/2}} \left[\frac{b_1^2}{0.64\ f'_c (N_2)^3} + \frac{N_4 N_1 b_1^3}{12.1\ d^2 f'_c (N_3)^2} \right] - 1.134\sqrt{f'_c}\, b_1^2$$

$$\frac{\partial G}{\partial b_2} = \frac{1}{(DENOM)^{3/2}} \left[\frac{b_2 h_2}{0.32\ f'_c (N_2)^3} + \frac{N_1 N_4 b_1 b_2 h_2}{6.05\ d^2 f'_c (N_3)^2} \right] - 2.268\sqrt{f'_c}\, b_2 h_2$$

$$\frac{\partial G}{\partial h_2} = \frac{1}{(DENOM)^{3/2}} \left[\frac{b_2^2}{0.64\ f'_c (N_2)^3} + \frac{N_4 N_1 b_1 b_2^2}{12.1\ d^2 f'_c (N_3)^2} \right] - 1.134\sqrt{f'_c}\, b_2^2$$

$$\frac{\partial G}{\partial d} = \frac{(N_4)^2}{d^3 (DENOM)^{3/2}}$$

$$\frac{\partial G}{\partial x_1} = 1.493 y_1 A_t f_y / s$$

$$\frac{\partial G}{\partial y_1} = 1.493 x_1 A_t f_y / s$$

$$\frac{\partial G}{\partial A_t} = 1.493 x_1 y_1 f_y / s$$

$$\frac{\partial G}{\partial f_y} = 1.493 x_1 y_1 A_t / s$$

$$\frac{\partial G}{\partial s} = -1.493 x_1 y_1 A_t f_y / s^2$$

$$\frac{\partial G}{\partial D_n} = - \frac{N_4}{10.71\ f'_c d^2 N_3 (DENOM)^{3/2}}$$

$$\frac{\partial G}{\partial L_n} = - \frac{N_4}{12.1\ f'_c d^2 N_3 (DENOM)^{3/2}}$$

Table A-2 gives the iteration results for Design No. 7.

TABLE A.2

Results for Design No. 7

Initial β = 2.00

Cycle No.	Variable	Initial x_i^*	$\partial G/\partial x_i^*$	α_i^*	New x_i^*
	f'_c	4700	-14708	-0.3004	5293
	b_1	14.00	-13510	-0.2883	14.36
	h_1	30.00	-7416	-0.1583	30.43
	b_2	5.00	-2672	-0.0570	5.03
	h_2	15.00	-1308	-0.0279	15.04
	d	27.5	2280	-0.0487	27.27
1	x_1	10.5	15503	0.3308	9.90
	y_1	26.5	15503	0.3308	25.00
	A_t	0.0696	6179	0.1319	0.0689
	f_y	64000	32083	0.6847	50855
	s	7.25	-13909	-0.2968	7.62
	D_n	60165	-1507	-0.0322	60552
	L_n	26563	-1472	-0.0314	26980
β = 1.8798					
	f'_c	5293	-14059	-0.2968	5251
	b_1	14.36	-13415	-0.2832	14.34
	h_1	30.43	-7362	-0.1554	30.39
	b_2	5.03	-2659	-0.0561	5.02
	h_2	15.04	-1301	-0.0275	15.03
	d	27.27	2276	-0.0481	27.29
2	x_1	9.90	15838	0.3343	9.93
	y_1	25.00	15838	0.3343	25.07
	A_t	0.0689	6329	0.1336	0.0690
	f_y	50855	32372	0.6834	51667
	s	7.62	-14285	-0.3016	7.60
	D_n	60552	-1507	-0.0318	60525
	L_n	26980	-1472	-0.0311	26951
β = 1.8797					

The vita has been removed from the scanned document